PONTIFICIA UNIVERSIDAD CATÓLICA DEL PERÚ

FACULTAD DE CIENCIAS E INGENIERÍA

Optimization of the alkaline treatment for *Agave americana* fiber and its influence on the mechanical properties of fly ash-based geopolymer

Tesis para obtener el título profesional de INGENIERA CIVIL

por

Shirley Melanie Rojas Clemente

Asesores

Suyeon Kim de Aguilar, PhD.

Coasesor: Rafael Aguilar Vélez, PhD.

Lima, mayo del 2021

Abstract

Geopolymers are good alternatives for replacing ordinary Portland cement (OPC) due to their comparable properties and feasibility to be obtained from industrial by-products. As OPC, geopolymers have superior compressive strength but a brittle behavior that the addition of fibers can improve. When the first macrocrack appears, fibers develop bridging mechanisms to allow the proper distribution of loads, so the composite can enable multiple cracks and enhance its ductility. At present, a wide range of materials can be used to reinforce cementitious matrices, from synthetics such as steel, glass, carbon, and polypropylene to natural fibers such as cotton, sweet sorghum, oil palm, coir, jute, sisal, flax, bamboo, etc. Natural fibers are among the most accepted resources to reinforce composites because they are biodegradable, renewable and generally, have a less environmental impact than their synthetic counterparts. They have low density and specific mechanical properties comparable to fibers made of glass, making them materials with a good performance-priceratio. However, their high variability of properties and hydrophilic behavior can create issues when reinforcing a matrix. Chemical treatments are used to clean chemical compounds that do not contribute to the fiber strength and favor moisture absorption. Aftertreatment, the fiber surface increases its roughness which enhances the interlocking within the composite. This thesis investigates the mechanical properties of *Agave americana* fibers obtained by beating and boiling the leaves. The fibers were subjected at 1%, 5%, and 20% NaOH concentrations over 0.5 hr, 1 hr, and 3 hr and tested to determine the tensile strength. The surfaces were also analyzed by scanning electron microscopy (SEM). After treatment, most of the fibers enhanced the tensile strength and strain and 1% NaOH concentration over1 hr was chosen as the optimum condition. Then, fibers were treated at the optimum condition and added to the geopolymer mixture at different doses: 0.5%, 0.75%, and 1% byweight of fly ash. The geopolymers were tested at compressive, flexural, and splitting tensile loads at 7 days of age. The compressive strength increased by 12% at 0.75 (wt.%) and the modulus of elasticity in compression, 13% at 1% (wt.%). Also, the tensile strength increased by 36% at 1 (wt.%). However, the flexural strength decreased probably due to the fiber length. Still, further studies are needed to understand the influence of the fiber length on the mechanical properties of geopolymers. Finally, the SEM analysis was conducted to identify the fiber failure modes

Acknowledgments

I want to acknowledge my supervisors, Prof. Suyeon Kim and Prof. Rafael Aguilar, for their availability, guidance and valuable discussions. Also, for their support of this idea and encouragement throughout the work. Thanks for motivating younger generations to get involved in science. To the Engineering and Heritage Research Group members, most of whom I got to know personally, thanks for your fellowship and enthusiastic support, which definitely, made this work more enjoyable. I want to thank Guido Silva and Jorge Salirrosas, who provided me with what I needed to know about the testing machines. And to Mauricio Gonzales, who authorized my entrances into the facilities whenever I needed them. Guido, Jorge, and Mauricio also made valuable suggestions while on the experimental stage of this work, which I truly appreciate. I want to express my sincere gratitude to Jorge for being an exceptional lab-mate who later became a very special friend, who helped my family and me during medical circumstances. And to Patricia Porcel, Rose Enciso, Steffi Huaranga, and Diana Zavaleta, hardworking girls whose dedication I could observe and were a huge inspiration to me and, for sure, to the following generations. I would also like to thank Luis-Felipe Sanchez, led by Prof. Javier Nakamatsu, for their ease and technical assistance when using the Chemistry Lab. Further, my appreciation to all I share a conversation about this thesis, each of whom made contributions that helped shape its structure. And to my friends Roberto, Carolina, Cesar, Lucero, and Emma for the great moments that make me reflect on the important things in life. Thanks for giving me so much without expectation. And finally, I would like to thank my family, the giant support in my life that inspires me to become a better version of myself. To my grandparents, both of whom instilled in me theimportance of education. My grandfather also shared his knowledge of the fiber manufacture used in this thesis. To my sister for ingraining in me a sense of independence but always making sure I stayed safe. To my uncle, who has significantly influenced my life, someone I have admired since a little child (no surprise, I chose this profession!). Thanks for sharing your passion for learning and for being available to me, no matter whenor what. And lastly, to my mother, the strength and motivation in my life. I know the sacrifices you made to give me opportunities that probably you did not have, for always ensured my education and health in such ways, I could never doubt of being loved.

Content

Content

- **LIST OF APPENDICES**

List of Figures

List of Figures

List of Figures

List of Tables

CHAPTER 1. Introduction

1.1 Background and justification for the study

According to the ACI, a fiber reinforcement system uses discontinuous discrete synthetic or natural fibers to reinforce a binder composed of hydraulic cement (American Concrete Institute, 2002). Similarly, in a fiber reinforced geopolymer system, the hydraulic cement is replaced with another type of binder obtained by the reaction of an alkali metal and an alumino-silicate mineral: a geopolymer. Since the raw minerals can be obtained from industrial by-products, geopolymers are known as greener alternatives; unfortunately, they also have brittle behavior.

Unlike reinforced concrete that uses steel bars to increase the strength of areas under tension, fibers aim to restrict the width of the cracks once the material exceeds the elastic zone (American Concrete Institute, 2002). For this reason, regardless of the kind of fiber used, fiber-reinforced composites do not necessarily enhance tensile strength; instead, they can develop greater ductility and fracture toughness compared to plain materials with brittle failure (Concrete Technology Weblog, 2008).

Since ancient times, humans have used fibers to manufacture building materials; such is the case of straw used to reduce cracks in walls built with adobe (Salih et al., 2020). At the end of the 19th century, asbestos was used as reinforcement for concrete on a commercial scale. Then, it would be restricted due to negative health effects. In 1950, researches were conducted on glass fibers to investigate the influence as reinforcement. However, fibers degraded under the concrete alkaline environment. Fortunately, this allowed the future development of alkali-resistant glass fibers. In 1960, researches began in the US to improve the properties of concrete by using steel fibers as reinforcement. In addition, investigations on natural fibers had the purpose of developing thin cement sheets for walls and floors to complement asbestos fibers. Later, in 1980 began the studies with natural fibers as an independent system of reinforcement for concrete (American Concrete Institute 2002). At present, cementitious matrices can be reinforced with natural and synthetic fibers.

Natural fiber cementitious composites can use a wide range of fibers such as cotton (Alomayri et al., 2014; Korniejenko et al., 2016), sweet sorghum (R. Chen et al., 2014), oil palm (Kroehong et al., 2018), hemp (Merta & Tschegg, 2013; Sedan et al., 2008), coir (Korniejenko et al., 2016; Yan, Chouw, et al., 2016), jute (Silva et al., 2020), sisal (Korniejenko et al., 2016; Silva et al., 2020), flax (Alzeer & MacKenzie, 2013; Lazorenko et al., 2020), bamboo (Sá Ribeiro et al., 2016), abaca (Malenab et al., 2017) and so on.

Natural fibers, however, have hydrophilic nature, which could cause mechanical interaction issues within the matrix. In addition, as they are not chemically inert, they can react with the geopolymer alkaline environment, compromising their durability. In order to counteract water absorption and improve fiber mechanical performance, chemical treatments have been developed.

One treatment for fibrillar surfaces is the alkaline treatment, which uses alkaline solutions to remove components from the fiber surface and decrease the hydrophilic character. The method also removes chemical components that disadvantage the fiber strength. In this way, fibers can be reoriented in the direction of the load and enhance their mechanical performance. Rocha et al. (2015) used the alkaline treatment on sisal fibers and removed amorphous constituents that were responsible for water absorption. Ajouguim et al. (2019) also verified the reduction of water absorption after treating Moroccan Alfa fibers. Their study also reports greater crystallinity and improved surface roughness. Cai et al. (2016) experimented with abaca fibers and obtained improved tensile strength and modulus of elasticity; however, the strain at break slightly decreased. Moreover, Thirumalaisamy and Pavayee Subramani (2018) used the treatment in agave Angustifolia Marginata fiber and found enhanced strength and improved crystallinity.

Agave americana is widely available in Peru, and the fibers could be obtained at low cost and energy. As reported in the literature, agave fibers were used to manufacture woven objects such as cordage, nets, mats, and clothing in our country since ancient times (Vallejos, 1982). Still, they could also be potentially suitable for reinforcing building materials. This study uses Agave americana fibers obtained by the boiling method and its optimization with alkaline treatment. Lastly, the influence of these fibers was studied in the mechanical properties of fly ash-based geopolymers. As far as this author knows, no chemical modification by alkaline treatment has been done on Agave americana fibers obtained by the boiling method and consequently use the fibers to reinforce geopolymers.

1.2 Research aims and scope

This thesis investigates the influence of alkali-treated Agave americana fibers to reinforce fly ash-based geopolymers as a contribution to natural fiber composite knowledge.

The specific objectives of the thesis are:

- Review of relevant scientific literature of geopolymers and natural fiber composites.

- Determine the mechanical properties of tensile strength and strain of natural and alkali-treated Agave americana fibers.
- Suggest an optimum alkaline treatment condition to improve the tensile strength of Agave americana fibers.
- Evaluate the mechanical properties of compressive, flexural, and splitting tensile strength of Agave americana fiber-reinforced fly ash-based geopolymers.
- Suggest a suitable fiber condition for the reinforcement of fly ash-based geopolymers.

The study will not evaluate the chemical composition and water absorption changes after the chemical treatment. Furthermore, the durability of the agave fibers within the alkaline environment of the composite is not part of the thesis.

1.3 Hypothesis

- After the alkaline treatment, Agave fiber will be able to reorient in the direction of load and increase its tensile strength. Due to the decrease in rigid behavior caused by the dissolution of amorphous chemical components, the strain of fibers is also expected to increase.
- After the reinforcement with fibers, geopolymers will shift the failure mode from brittle to ductile. Besides, because fibers will bridge the cracks once superseded the elastic zone, a certain increase in the material strength could also be expected.

1.4 Structure of the thesis

This thesis is composed of six chapters:

Chapter 1: Introduction to the study composed of background and justification, research aims and scope, hypothesis, and structure.

Chapter 2: Development of the state-of-art of fly ash-based geopolymers. The raw materials, stages, and factors that influence geopolymerization and also the physical properties of geopolymers are described.

Chapter 3: Development of the state-of-art of natural-fiber reinforced geopolymers where

the chemical composition, physical and mechanical properties, and factors that influence the fiber properties are described. This chapter also introduces the alkaline treatment and the fiber content in cement composites.

Chapter 4: Development of the mechanical characterization of natural and alkali-treated Agave americana fibers. This chapter develops the experimental plan, results, and discussion.

Chapter 5: Development of the mechanical characterization of fly ash-based geopolymer reinforced with alkali-treated Agave americana fiber. This chapter develops the experimental plan, results, and discussion.

Finally, Chapter 6 presents the conclusions and recommendations for the study.

CHAPTER 2. Fly ash-based geopolymers

Abstract. This chapter reviews the state-of-art of fly ash-based geopolymers. Geopolymers are a type of cementitious material obtained by solid alumino-silicate minerals and alkali reagents at low temperatures. The solid alumino-silicates can be natural or industrial by-products like fly ash, a by-product of power plants that use coal as an energy source. The type of fly ash influences the properties of the geopolymers. Some of them are the chemical composition and particle size gradation, so the nature of the alkaline reagent and its concentration, which has to be high enough to promote the dissolution of chemicals but not too high to hinder the polycondensation of partial products. Curing conditions such as time and temperature need to be considered because they can favor the dissolution rate and prevent voids in the matrix. In contrast to OPC, fly ash based-geopolymers have superior performance under fire exposure and chemical erosion. The geopolymerization reaction is an effective method for the immobilization of the toxic elements from the fly ash.

2.1 Introduction

OPC is a major construction material that requires high amounts of energy to be manufactured- This industry releases about 8% of the CO_2 worldwide emissions each year (Andrew, 2019). The replacement of fossil fuels and modern technologies could reduce emissions, but the calcination of limestone inherently produces greenhouse gases. Therefore, the development of materials with a similar performance obtained at a comparable cost has been of interest during the last decades.

Geopolymers are cementitious materials with a ceramics-like appearance whose denomination comes in analogy to the natural process of geosynthesis from which most of the Earth's crust was formed; for that reason, they are also known as human-made rocks (Davidovits, 1994). There is evidence that ancient civilizations like the Egyptians and Tiahuanacos knew this technology and employed the geopolymerization reaction to manufacture construction materials and ornamental objects (Davidovits, 2008; Davidovits, Huaman & Davidovits, 2019)

Geopolymers are inorganic polymers obtained at low temperatures, generally below 100°C, mainly composed of nanoparticles in the range of 5 nm to 15 nm. Depending on the raw material, the chemical structures include silico-oxide (-Si-O-Si-O-), silico-aluminate (-Si-O-Al-O-), ferro-silico-aluminate (-Fe-O-Si-O-Al-O-), and alumino-phosphate (-Al-O-PO-) units (Davidovits, 2017). The Si:Al ratio is a parameter that determines the properties of geopolymers, low ratios of 1 to 2 form a three-dimensional rigid structure, but as the Si:Al ratio increases, a transition from a three-dimensional to a two-dimensional structure takes place, as observed in Figure 2.1.

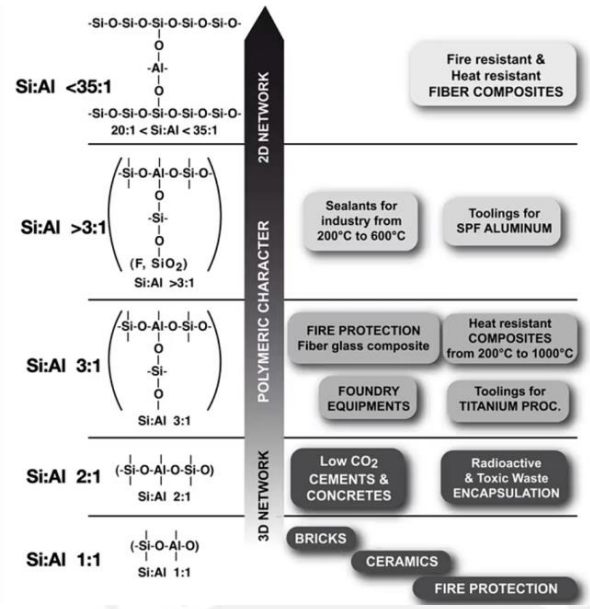

Figure 2.1 Chemical structures for silico-aluminate geopolymers and their application (Geopolymer Institute, 2020).

The first geopolymer was obtained in 1978 from the reaction of metakaolin and sodium hydroxide (NaOH) in aims to find a replacement for flammable organic resins. It was used as a building panel coating commercially known as Geopolymite™. In 1983, Lone Star Industries and Shell Oil Company developed the first polymer cement from calcium silicate, blast furnace slag, and organic polymers. It was known as Pyrament®, composed of 20% geopolymer and 80% Portland cement, could develop early compressive strengths of 20 MPa in four hours (Davidovits, 1994).

Nowadays, geopolymers have a wide range of applications, including aerospace, automobile, plastic, metallurgy, medical, and construction sectors. Geopolymers used in the construction sector may have a Si:Al ratio in the range of 1 to 2, but ratios of 2 to 3.5 are suggested for road infrastructure (Federal Highway Administration [FHWA], 2004). Two important cases for the applications are the Global Change Institute (2013) at the University of Queensland and The Brisbane West Wellcamp airport (2014), both located in Australia. The projects used fly ash and blast-furnace slag geopolymers.

2.2 Raw materials

The raw materials of geopolymers are solid alumino-silicate minerals and alkali reagents. Solid alumino-silicates have a rich chemical composition in silica (SiO_2) and alumina (Al_2O_3). They are commonly used as supplementary materials in the Portland cement industry to react with the excess of calcium hydroxide, $Ca(OH)_2$, and produce C-S-H gel in order to increase the compressive strength (Imbabi, Carrigan & McKenna, 2013; Zhuang et al., 2016). Table 2.1 shows the chemical composition of raw minerals used to produce geopolymers. They can be natural minerals, such as kaolinite, laterites, or volcanic rocks, and industrial by-products such as fly ash, blast furnace slag, mining tailings, rice husk ash, or red mud. Some of them may require pre-treatments before use, such as kaolinite and rice husks, that must undergo physical processes such as calcination. The reagents can be alkali hydroxides like NaOH, KOH, $Ca(OH)_2$, or silicate solutions Na_2SiO_3, which are used to provide a medium of alumino-silicate dissolution.

Table 2.1: Chemical composition of alumino-silicate mineral sources.

Material	SiO_2	Al_2O_3	Fe_2O_3	K_2O	CaO	TiO_2	MgO	Na_2O	SO_3	NaOH	$NaAlO_2$	LOI	Others
Bottom ash (Chindaprasirt, Jaturapitakkul, Chalee & Rattanasak 2009)	38.8	21.3	12.1	2.5	16.5	0.8	1.7	1.0	2.4			2.9	
Fly ash (Coal origin: Anthracite and soft coal) (Fernández-Jiménez & Palomo, 2003)	53.09	24.80	8.01	3.78	2.44	1.07	1.94	0.73	0.23	-	-	3.59	0.55
Fly ash (Coal origin: Soft coal and lignite) (Fernández-Jiménez & Palomo, 2003)	42.62	29.21	16.77	1.13	6.37	-	1.35	0.19	0.42			1.63	
Mine tailings (Ahmari & Zhang, 2012)	64.8	7.08	4.33	3.26	7.52	-	4.06	0.90	1.66	-	-	-	-
Blast furnace slag (Cheng & Chiu, 2003)	34.39	14.47	0.63	0.36	41.67	0.53	6.49	0.22	-	-	-	-	<0.01
Metakaolin (Cheng & Chiu, 2003)	52.26	42.83	1.01	1.56	0.02	0.13	0.09	0.02	-	-	-	-	<0.01
Rice husk ash (He, Jie, Zhang, Yu & Zhang, 2013)	91.5	-	-	2.3	-	-	-	-	-	-	-	-	6.0
Red mud (He et al., 2013)	1.2	14.0	30.9	-	2.5	4.5	-	-	-	20.2	23.0	-	1.7

2.2.1 Fly ash

Fly ash is a by-product of power plants, an industry that consumes 40% of the world's available coal, according to the International Energy Agency (IEA, 2019). Fly ash represents about 64% of the coal combustion products (Figure 2.2a) and is mainly used as a concrete addition (Figure 2.2b). Their particles are generally recovered from the flue gases by electrostatic precipitation (Ahmaruzzaman, 2010; Gorai et al., 2006, as cited in Zhuang et al., 2016). Their chemical composition is mainly constituted of SiO_2, Al_2O_3, and FeO_3, as observed in Table 2.1. The ASTM C618 (ASTM International, 2019) classifies the fly ash into two types: Class C and Class F, according to the CaO content (Table 2.2). The use of low calcium, Class F, fly ash is suggested since high amounts of calcium may interfere in the geopolymerization process and physical properties (Gourley, 2003, as cited in Hardjito & Rangan, 2014).

Table 2.2: Difference between Class C and Class F fly ash, according to the ASTM C618 (ASTM International, 2019).

Item		Class C	Class F
Source[1]		Burning lignite or subbituminous coal	Burning anthracite or bituminous coal
Chemical composition	$SiO_2 + Al_2O_3 + Fe_2O_3$ (%) (min)	50	
	CaO (%)	>18	<18
	SO_3 (%) (máx)	5	
Moisture content (%) (máx)		3	
Loss on ignition (L.O.I.) (%) (máx)		6	

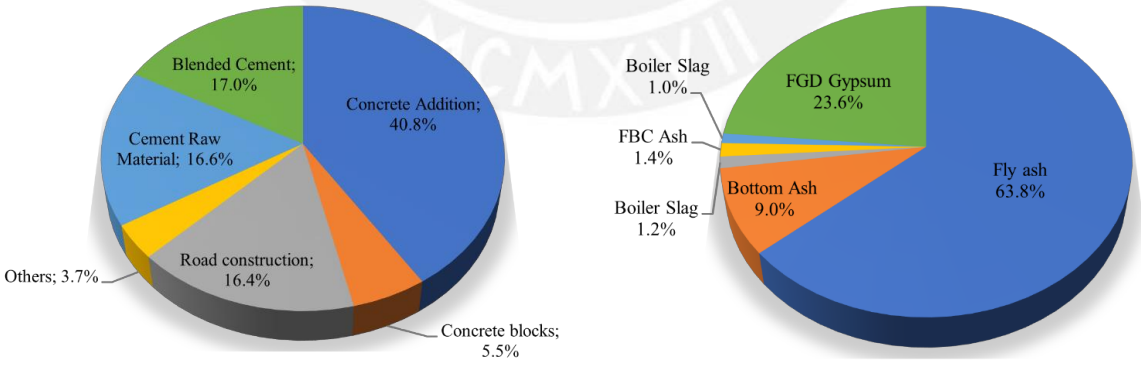

(a) **(b)**

Figure 2.2 (a) Production of coal combustion products and (b). use of fly ash in the construction industry. (European Coal Combustion Products Association [ECOBA], 2016).

2.3 Synthesis of geopolymers

2.3.1 Stages

Geopolymerization consists of the three following stages:

> (i) dissolution of the oxidized minerals present in the raw material (usually silica and alumina) under highly alkaline conditions, (ii) transport/orientation of the dissolved oxidized minerals followed by coagulation and gel formation, and (iii) polycondensation to form a three-dimensional network of aluminosilicate structures (Silva, 2007, as cited in Silva, 2018).

Figure 2.3 shows the process of geopolymerization of blast-furnace slag. Gehlenite (Figure 2.3a) and akermanite (Figure 2.3b) are the main minerals of the raw material. The dissolution begins at alkaline mediums, where the gehlenite forms the (K, Ca)-ortho-sialate-hydrate molecule and aluminum hydroxide $Al(OH)_3$ (Figure 2.3c). Akermanite depolymerizes into Ca-di-siloxonate hydrate and magnesium hydroxide $Mg(OH)_2$ (Figure 2.3d). The two molecules interact and form a (K,Ca)-cyclo-ortho (sialate-disiloxo) and Ca-di-siloxonate-hydrate system (Figure 2.3e) (Geopolymer Institute, 2014, 0:27-4:20).

Whereas this step is the last stage of geopolymerization or represents the end of the alkali-activation is a point of discussion. According to Davidovits, the potassium is outside the molecule (Figure 2.3e), making it susceptible to leaching. However, geopolymers of three-dimensional structures do not have leaching issues that can compromise the durability; therefore, it represents a gel of an unknown structure that needs to interact with a source of alumino-silicate to form a geopolymer (Geopolymer Institute, 2014, 2:40-4:35). Other authors have mentioned the addition of mineral sources to reduce the setting time (Hardjito & Rangan, 2014). A detailed discussion about the chemistry of alkali-activation and geopolymerization is beyond the scope of this review.

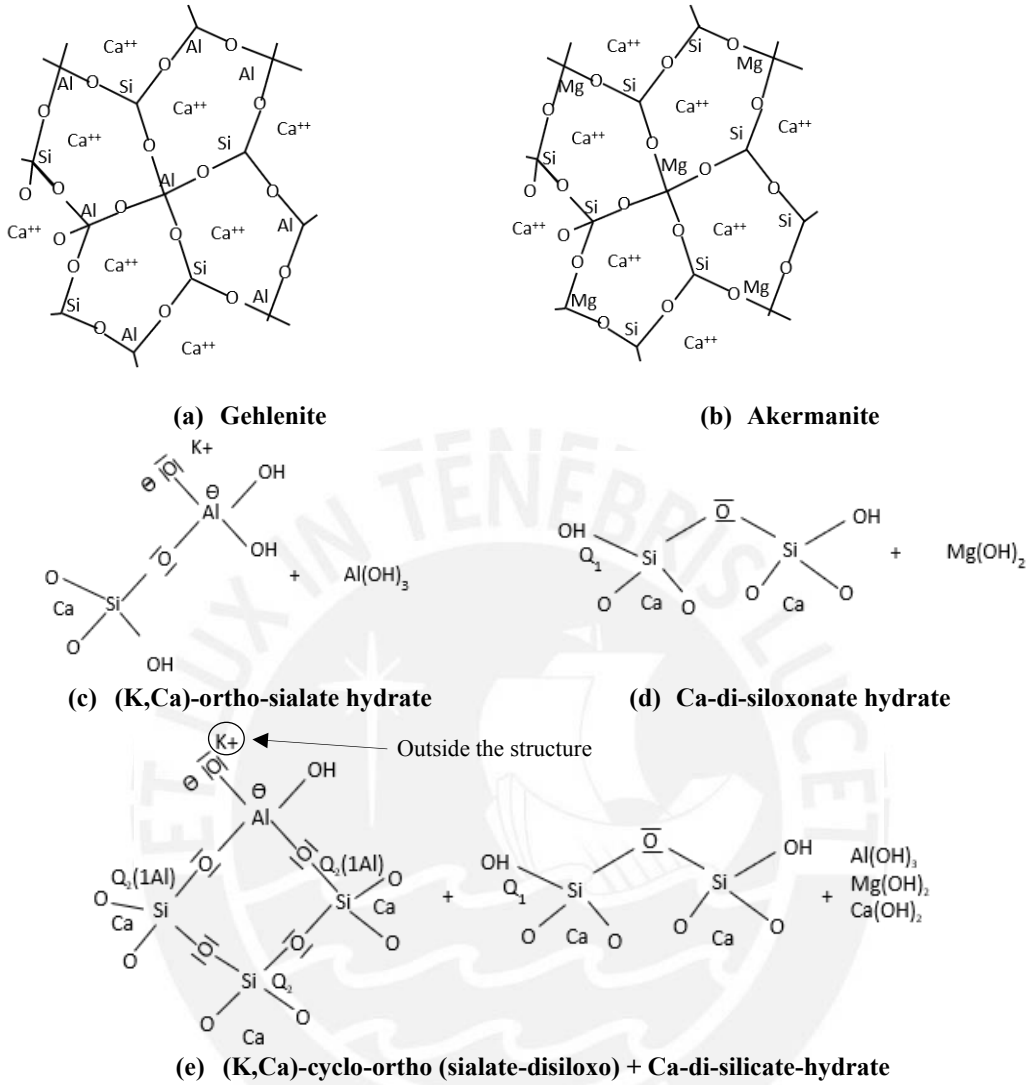

Figure 2.3. Alkali-activation process for blast-furnace slag: (a), (b) chemical structure of gehlenite and akermanite; (c), (d) dissolution of alumino-silicate minerals in alkali medium and (e) (K,Ca)-ortho-sialate-hydrate and Ca-di-siloxonate hydrate condensation (Geopolymer Institute, 2014, 0:27-4:20).

2.3.2 Factors influencing the geopolymerization process

The properties of the solid alumino-silicate minerals and the alkaline reagents used to obtain the geopolymer influence the chemical process. For fly-ash based geopolymers, the chemical composition of the fly ash, such as the content of amorphous or crystalline phases, and its physical properties, such as the particle size, play an essential role in the determination of properties (Fernández-Jiménez & Palomo, 2003); but also the nature and concentration of the alkaline reagent and curing conditions such as time and temperature (Komljenović, Bascarević & Bradić, 2010; Zhuang et al., 2016).

a. Chemical and physical properties of fly ash

Fly ash is constituted of glassy phases mainly composed of aluminates and silicates (Görhan & Kürklü, 2014), and minor crystalline phases composed of mullite, quartz, magnetite, hematite, feldspar, anhydrite, and calcite (Komljenović et al., 2010). In the geopolymerization process, the glassy phase reacts in contact with alkaline mediums and favors the dissolution rate. If the rate is high enough, fewer crystals are formed in the alumino-silicate product (Fernández-Jiménez & Palomo, 2003), increasing the compressive strength (Komljenović et al., 2010). However, depending on the alkaline reagent and the experimental conditions, the product could develop additional crystalline phases (Fernández-Jiménez, Palomo & Criado, 2006). On the other hand, a high content of loss on ignition (LOI) can negatively impact the geopolymer properties. LOI represents the unburned carbon residue content (Wattimena & Hardjito, 2017) which is characterized for having a low chemical activity (Sagawa et al., 2015). A high LOI content demands water use, and consequently, affects the compressive strength of the geopolymer (Wattimena & Hardjito, 2017). The ASTM C618 indicates a maximum LOI content of 6% by weight for C and F class fly ash (ASTM International, 2019). Sagawa et al. (2015) used a high LOI (9%) and a Class F fly ash to prepare geopolymer mortars. The compressive strength of Class F fly ash geopolymer mortars obtained 30% to 50% higher values than that of the high LOI fly ash mortar.

On the other hand, some physical properties of the fly ash, such as particle size larger than 43 μm, are less active in the geopolymerization reaction and decrease the dissolution rate (Komljenović et al., 2010). If this criterion is exceeded, methods like milling could reduce particle size (Mejía, Rodríguez & De Gutiérrez, 2014). Fernández-Jiménez & Palomo (2003) evaluated the compressive strength of geopolymers obtained from several fly ash types. Those matrices constituted of fly ashes with a higher silica content, and particle size minor than 45 μm had higher compressive strength.

b. Nature and concentration of alkaline reagents

According to the literature, the dissolution of fly ash minerals occurs faster when the OH^- concentration is high enough (Görhan & Kürklü, 2014), and higher concentrations have a positive influence on the compressive strength (Hardjito & Rangan, 2014); however, an excess of alkalinity could have adverse effects because it can hinder the polycondensation of partial products (Görhan & Kürklü, 2014). Komljenovic' et al. (2010) evaluated the

influence of potassium hydroxide (KOH), sodium hydroxide plus sodium carbonate (NaOH+Na2CO3), sodium hydroxide (NaOH), and soluble silicates (Na2O.nSi2O2) in the fly ash geopolymerization. The results showed that the compressive strength of the geopolymers increased from using potassium hydroxide to soluble silicates as alkaline reagents. When working with sodium hydroxide (NaOH) and potassium hydroxide (KOH), the size of the ions influences the geopolymerization rate. Although sodium is less reactive than potassium, the geopolymerization is more effective with NaOH due to the ion's smaller size (Davidovits, 2015). Using carbonated solutions is not recommended when working with fly ash because they produce acid media and impair the reaction (Fernández-Jiménez & Palomo, 2003). On the other hand, alkali reagents like soluble silicate contain partially polymerized silica and enhance the matrix compactness and mechanical performance (Fernández-Jiménez et al., 2006).

c. Curing conditions as time and temperature

According to Sindhunata, Van Deventer, Lukey & Xu (2006), the curing time is one factor that positively influences the compactness of fly ash-based geopolymers because it increases the rate of reaction. For the study, geopolymers cured at 75°C obtained fewer pores (Figure 2.4a) than those cured at 30°C (Figure 2.4b). Hardjito & Rangan (2005) studied the effect of curing times of 4 hr to 96 hr in the compressive strength of fly ash-based matrices suggesting that a significant increase in the mechanical properties occurs until the first 24 h; therefore, for practical applications, it is not necessary to prolong the curing time more than one day.

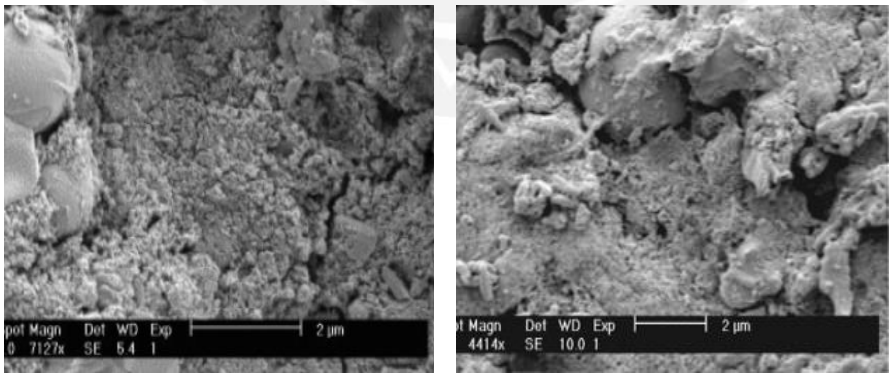

(a) **(b)**

Figure 2.4 Scanning electron microscope (SEM) of fly ash-based geopolymers cured at (a) 75°C and (b) 30°C. According to Sindhunata et al., (2006), the matrix cured at 75°C showed higher compactness than the other cured at 30°C.

2.4 Physical properties of fly-ash based geopolymers

2.4.1 Immobilization of toxic materials

Martínez, Mejía, Torres & Mejía, (2015) evaluated the effectiveness of the immobilization of toxic elements of the fly ash. Class F fly ash-based geopolymers were subjected to the leaching process, and the concentration of heavy metals: Cr, V, Zn, Ni, As, Ba, Sr, Pb, and Cd were analyzed. Most metals, except for V and As, were immobilized effectively and complied with drinking water regulations. Palomo & Palacios (2003) studied the immobilization of Cr and Pb for Class F alkali-activated geopolymer and OPC. Even though the alkali-activated product stabilized Pb effectively, it was unable to solidify Cr; in comparison to OPC, where the Cr becomes part of the structure and increases its mechanical performance. Van Jaarsveld & Van Deventer (1999) mentions that the immobilization of toxic elements depends on factors such as the radius of the metal ions, the nature of the alkaline reactant, and the source of alumino-silicate minerals.

2.4.2 Alkali silica reaction (ASR)

Alkali silica reaction (ASR) occurs between hydroxyl ions from the concrete and the silica minerals from the aggregates having negative consequences, such as expansion, cracking, and strength loss of the composite. Kupwade-Patil & Alloche (2013) evaluated the alkali-silica reaction on OPC, Class C, and Class F fly ash-based geopolymer identifying cracks and ASR gel on the OPC (Figure 2.5a) and Class C geopolymer. No signs of ASR were identified on the Class F specimen (Figure 2.5b); and compared to the geopolymers, OPC showed higher volume expansion, which would indicate they are more vulnerable to ASR.

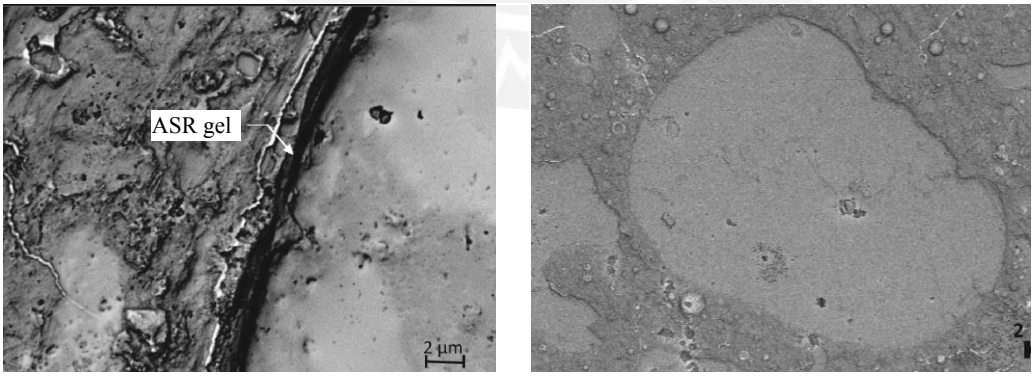

(a) **(b)**

Figure 2.5. Scanning electron microscope (SEM) of (a) OPC and (b) class F fly ash-based geopolymer. No signs of alkali-silica reaction (ASR) gel were observed on the geopolymer (Kupwade-Patil & Alloche, 2013).

2.4.3 Resistance to fire exposure

Sarker, Kelly & Yao (2014) compared the effects of fire exposure at 400, 650, 800, and 1000°C on fly ash-based geopolymers and OPC. At higher temperatures of 800 and 1000°C, OPC suffered spalling and considerable cracks appeared on the surface. The samples retained between 11% to 16% of their compressive strength, while geopolymers showed better resistance, retaining 21% to 29%; therefore, showing better performance to spalling and cracking after exposure to high temperatures.

2.4.4 Chemical resistance

Fly ash-based geopolymers have good resistance to acid and chloride erosion, according to Zhuang, Zhang & Xu (2017), who evaluated the mechanical performance of fly ash geopolymers subjected to sodium chloride and sulfuric acid at 360 days of exposure. For this study, geopolymers exhibited a 6% decrease in flexural, 11% in compressive, and 15% in tensile strength. Sukmak, De Silva, Horpibulsuk & Chindaprasirt (2015) compared the physical performance of clay-fly ash-based geopolymer and clay-cement under sulfate-rich conditions. Even though the sulfate impacts the degradation rate, the clay-fly ash geopolymer was less susceptible to sulfate attacks than the traditional clay-cement system.

CHAPTER 3. Natural fiber reinforced cementitious composites

Abstract. This chapter reviews the state-of-art regarding natural fiber-reinforced geopolymers. Natural fibers have become sustainable options due to their good mechanical properties, low environmental impact, and economic value compared to synthetic fibers. They can be obtained from the bast, leaf, seed, and stalks of plants through mechanical, biological and chemical methods or a combination of them. Plant fibers are a composite by nature because the cellulose fibrils are embedded in a matrix of hemicellulose, lignin, pectin, and waxes. Some of the factors influencing the fiber mechanical properties are the cellulose content, its degree of crystallinity, fiber morphology, microfibrillar angle (MFA). On the other hand, working with natural fibers entails some disadvantages, such as the high variability of properties and a hydrophilic nature that creates issues when they reinforce a matrix. Chemical treatments clean non-cellulosic compounds, after which the fiber can enhance its strength because cellulose fibrils can be able to rearrange. They also modify the hydrophilic nature, improving the interfacial bonding between the fiber and the matrix, thus enhancing the mechanical properties of the composite.

3.1 Introduction

Natural fibers are among the most accepted resources for reinforcing composites because they are biodegradable, renewable and abundant materials. Most fibers require less energy to be produced which makes then cheaper than fibers such as steel, glass or carbon (Ramamoorthy et al., 2015). Generally, they have low density making them attractive for reinforcing structures when weight is a consideration (Djafari Petroudy, 2017). Natural fibers have specific mechanical properties similar to those of artificial fibers such as glass (Djafari Petroudy, 2017), so their performance-price ratio (modulus/cost) is higher than that of artificial fibers (Ramamoorthy et al., 2015).

Natural fibers englobe animals, minerals and plants (Figure 3.1). Animal fibers are the second most important source of natural fibers after plant fibers. They are mainly composed of protein and could be obtained from the secretion of insects, e.g., silk, wool or hair and feathers from birds (Gholampour & Ozbakkaloglu, 2019). Except for bird feathers which are usually waste, animal fibers are more expensive than plant fibers (Ramamoorthy et al., 2015). Asbestos represents mineral fibers, but its use is restricted because of its danger to human health. Other mineral sources for natural fibers are Wollastonite and basal (Löfgren, 2005).

Plant fibers act as a reinforced system by nature where the non-cellulosic components such as hemicellulose, lignin, pectin, and waxes wrap the cellulose fibrils (Ray & Sarkar, 2001). In comparison to animal fibers, plant fibers have good resistance to alkalis and a higher stiffness (Gholampour & Ozbakkaloglu, 2019). They are biodegradable, cost-effectively, non-hazardous, (Yan, Kasal, et al., 2016) and can be obtained from the bast; leaves, seeds, fruits, wood, stalks, and grass (Figure 3.1).

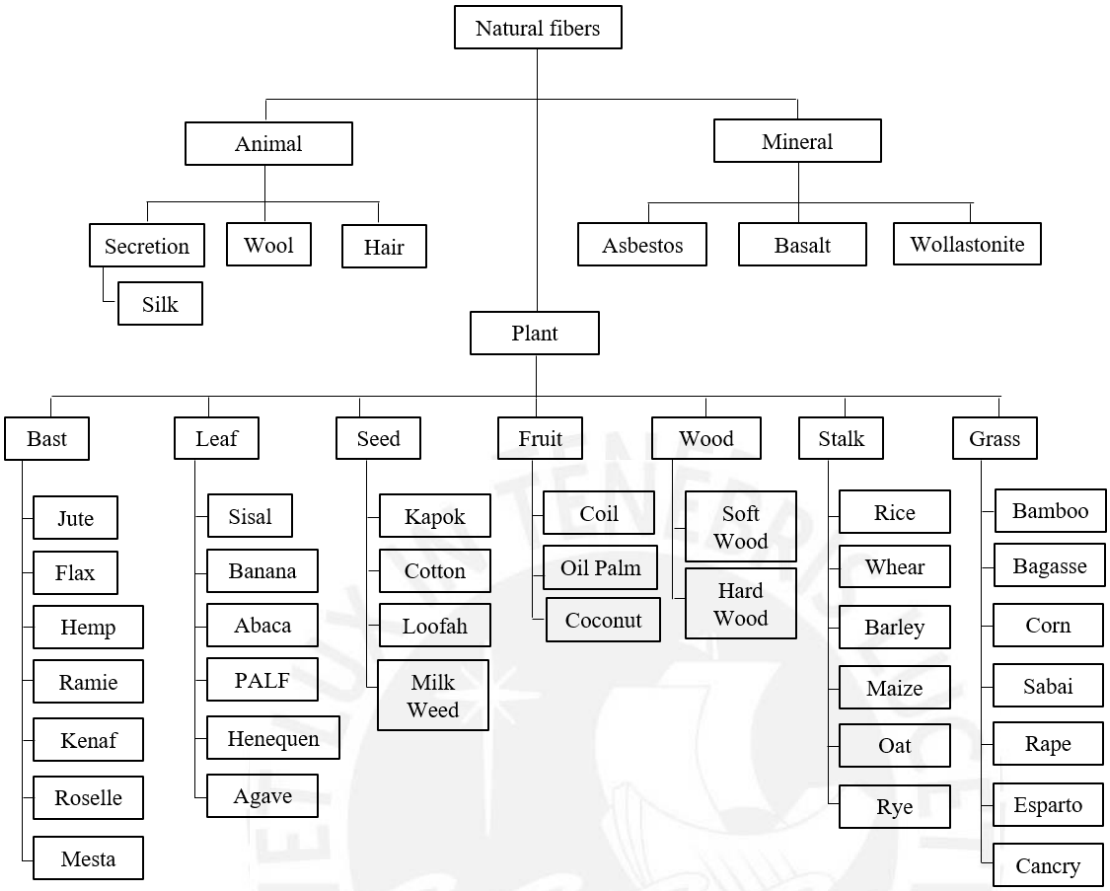

Figure 3.1 Sources for natural fibers (Modified from Jawaid & Abdul, 2011, as reproduced in Yan, Kasal & Huang, 2016).

One of the major concerns when working with plant fibers is the hydrophilic behavior caused by chemical compounds such as hemicellulose, lignin, pectin, and amorphous cellulose regions (Célino et al. 2014). The absorption of water causes fiber swelling, and its evaporation produces fibers shrinkage. This mechanism induces stresses in the interface, produces cracks and the loss of contact between the fiber and the cementitious matrix (Camargo et al., 2020; Yan, Kasal, et al., 2016). Also, the high variability of chemical composition and physical properties like diameter, length, and roughness are other shortcomings when working with these fibers (Yan, Kasal & Huang, 2016). Table 3.1 lists other issues among some benefits of natural fibers.

Table 3.1 Benefits and shortcomings of natural fibers (Adapted from Pickering et al., 2016).

Benefits	Shortcomings
Low density, high specific strength, and stiffness.	Lower durability than synthetic materials. May require treatment.
Renewable resources. Little energy required for production.	High moisture absorption. The swelling and drying process leads to mechanical interfacial issues.
Lower cost than synthetic fibers.	Lower strength and impact strength compared to synthetic fiber composites.
Low hazard manufacturing processes.	High scattering of properties.
Low emission of toxic fumes when subjected to heat.	Lower processing temperatures limit matrix options.

Fiber obtention consists of the separation of fiber bundles through a partial decomposition of the cell wall (Amel et al., 2013) through mechanical, biological, enzymatic, chemical procedures, as well as their combination. Mechanical procedures use tools to break the stalks, scutch and hackle the fibers. Decorticators or elements such as wood rollers or stones could also be used, e.g., high Andean communities of Peru use stones to manufacture ichu fibers (Roel, Hernández & Huamaní, n.d.). Biological methods, also known as retting, use microorganisms such as fungi and bacteria to degrade the vegetal crust being dew and water retting the most popular. Water retting consists of soaking the fibers into the water for at least 7 to 14 days prior to developing bacteria, while dew retting consists of leaving the plants for several weeks (up to ten) at fields at the action of microorganisms (Sisti et al., 2018). Dew retting is restricted to areas with suitable climatic conditions that allow the procreation of microorganisms and has a high risk of fiber contamination with soils. In the case of water retting, high-quality fibers could be obtained, but the method consumes large amounts of water (Lee et al., 2020). Moreover, as Jankauskiene and Gruzdeviene (2013) described, these methods could also employ mechanical procedures such as combing the fibers after the microbiological action. Enzymatic retting is similar to water retting but adds enzymes to the water to hydrolyze pectin and gums. It has decreased extraction time that water retting and could last from 8 hr to 24 hr (Lee et al., 2020; Sisti et al., 2018). There are also chemical methods that consist of submerging the plants in alkali or acid solutions to promote fibrillation (Gomez, 2015) and could allow the obtention of high-quality fibers in shorter times (Sisti et al., 2018). Chemical treatments could be applied under variable conditions of temperature and pressure.

3.2 Plant fiber properties

3.2.1 Chemical composition

Plant fibers are mainly composed of cellulose, hemicellulose and lignin (Célino et al., 2014b), but generally, cellulose is the main structural component between 40% to 45% of the chemical composition (Djafari Petroudy, 2017). It is a strong, rigid molecule of carbon, hydrogen, and oxygen bonded by hydroxyl groups, relatively unaffected by alkalis and dilute acids (Djafari Petroudy, 2017). Its content is related to mechanical properties such as tensile strength and modulus of elasticity (Yan, Chouw, Huang & Kasal 2016). Because cellulose can adopt a crystalline and amorphous character is semicrystalline (Célino et al., 2014a).

Hemicellulose is an amorphous polymer, soluble in water, composed of hydroxyl and acetyl groups (Yan, Kasal, et al., 2016) that makeup networks with cellulose through hydrogen bonds (Liu, Mohanty, Drzal, Askel & Misra, 2004). Lignin is an aromatic amorphous polymer that provides plants a rigid behavior which is why they can reach considerable heights. (Yan, Kasal, et al., 2016). Covalent bonds join lignin and hemicellulose, and their content is related to water absorption capacity. Pectin is constituted of polar carboxyl groups and is located in the middle lamella of plant fibers, a transition zone between elementary fibers that composed a fiber bundle.The middle lamella can be a preferential water path when plant fibers are subjected to moisture (Célino et al., 2014b). Finally, waxes also make part of the fiber composition and can be an obstacle for fiber and matrix adherence (Yan, Chouw et al., 2016). Table 3.2 shows the chemical composition of several plant fibers.

Table 3.2 Chemical composition of plant fibers (El Oudiani, Ben Sghaier, Chaabouni, Msahli & Sakli, 2012; Gholampour & Ozbakkaloglu, 2019; Mori, Tenazoa, Candiotti, Flores & Charca, 2018).

Fiber	Cellulose (%)	Hemicellulose (%)	Lignin (%)	Waxes (%)
Abaca	56–63	20–25	7–9	3
Agave americana	65	32	3	-
Coir	32–43	0.15–0.25	40–45	–
Cotton	85–90	6	–	0.6
Flax	71	19–21	2	1.5
Jute	61–71	14–20	12–13	0.5
Kapok	64	23	–	–
Kenaf	72	20	9	–
Bamboo	26–43	30	21–31	–
Hemp	68	15	10	0.8
Pineapple	81	–	13	–
Ramie	67–76	13–16	0.6–0.7	0.3
Sisal	65	12	10	2
Bagasse	55.2	17	25	–
Oil Palm	65	–	29	–
Curaua	74	10	8	–
Wheat (straw)	38–45	15–31	12–20	–
Rice (straw)	41–57	33	8–19	8–38
Ichu	37-43	25-30	13-16	-

3.2.2 Physical and mechanical properties

Elementary plant fibers are structured as primary and secondary concentric cell walls of different thicknesses (Figure 3.2a). Primary walls are the exterior layers, usually composed of pectin, low crystalline cellulose, hemicellulose and waxes. Secondary walls (S1, S2 and S3) represent about 90% of the cell wall thickness and are composed of cellulose microfibrils. The secondary layer S2 represents between 70% to 80% of the thickness; therefore, fiber properties depend on it (Célino et al., 2014b). Generally, each fiber locates a small channel known as lumen in its center (Figure 3.2b), responsible for the water uptake. Due to their hollow structure, plant fibers have a lower density than synthetic fibers making them an attractive option to reinforce composites if the weight represents a concern (Djafari Petroudy, 2017). However, it also causes water to be trapped inside the pores (Célino et al., 2014b).

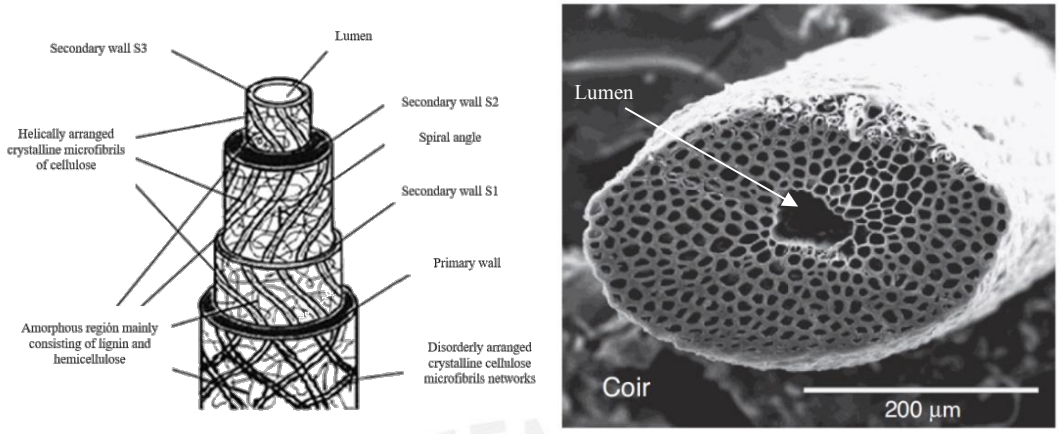

Figure 3.2 Morphology of plant fibers (a) structure of an elementary fiber (Gholampour & Ozbakkaloglu, 2019), (b) lumen observed in a cross-section of a coir fiber (Alves Fidelis, Pereira, Gomes, de Andrade Silva & Toledo, 2013).

Cellulose crystallinity is another property that determines the mechanical performance since it has a greater stiffness than other chemical components: the more crystalline this molecule, the greater the fiber strength. However, a lower crystallinity allows the fiber to elongate more (Djafari Petroudy, 2017). Microfibrillar angle (MFA) is the angle formed between the cellulose microfibrils and the plant fiber axis. Generally, non-wood fibers have MFA values between 6°-10°. But, fibers like coir have an MFA value of 45°, which is high compared to other non-wood fibers like flax, whose angle is reported at 10° (Yan, Chouw, et al., 2016). Mechanical properties such as stiffness and strength are susceptible to this parameter and generally show an inversely proportional relationship. For this reason, coir fibers have lower tensile strength than flax fibers, as shown in Table 3.3. When the MFA is small and the content of cellulose suitable, fibers present high stiffness and strength. When the MFA is high, ductility increases because they can twist when stretched (Djafari Petroudy, 2017).

Natural fibers used as reinforcement are classified into two groups: (i) short fibers between 1 mm-5 mm usually employed as randomly oriented (Figure 3.3 [a], [b], [c], and [d]), whose compounds acquire isotropic character, and (ii) long fibers between 5 mm-50 mm used for one direction reinforcement (Figure 3.3 [e] and [f]), which gives the composite anisotropy character (Djafari Petroudy, 2017). Unlike synthetics, natural fibers are irregular in both transverse and longitudinal directions, as shown in Figure 3.4 (b) and (c) (Löfgren, 2005). The ratio between length and diameter defines the aspect ratio, one of the most influential parameters to determine mechanical properties. At the ends of the fiber, the stresses are zero

and increase along its length (Pickering et al., 2016). The critical length is the shortest length that allows the fiber to be fully loaded before failing, as long as there is adequate adhesion between the elements of the composite. To allow the proper transfer of stresses, prevent the low dispersion of fibers, and act only as a filler, the fiber length should ideally be greater than the critical length (Djafari Petroudy, 2017).

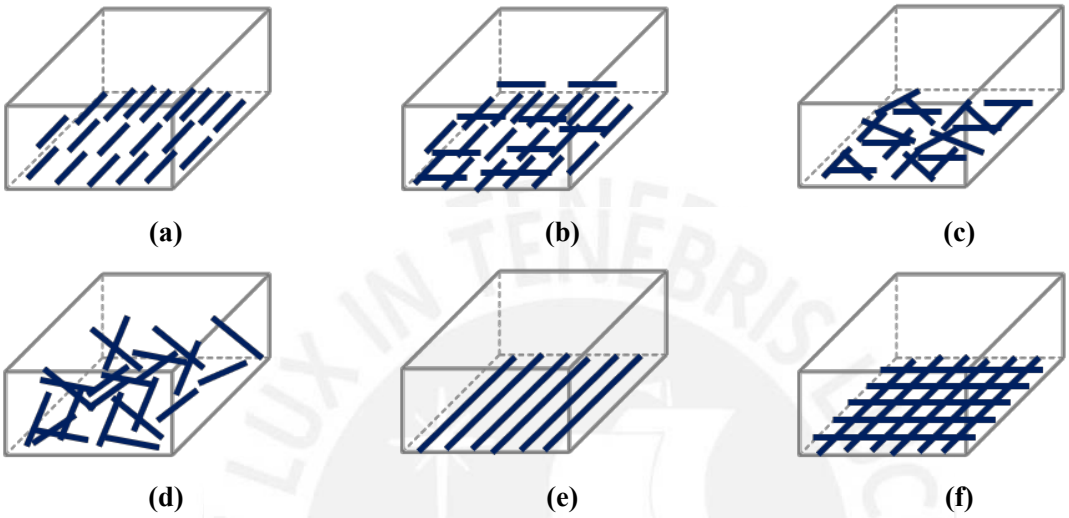

Figure 3.3 Fiber arrangement in reinforced composites: discontinuous fibers (a) 1-D fibre orientation, (b) 2-D fibre orientation, (c) plane-random orientation and (d) random fibre orientation and continuous fibers (e) unidirectional, (f) bi-directional (Adapted from Löfgren, 2005).

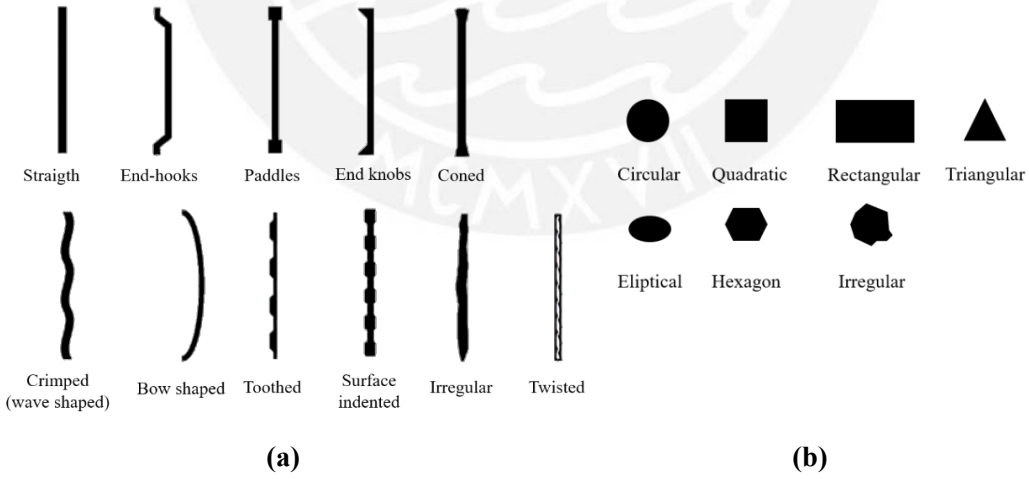

Figure 3.4 Typical geometries of fibers used in reinforced composites: (a) longitudinal geometry and (b) diameters (Adapted from Löfgren, 2005).

Table 3.3 shows some physical and mechanical properties of natural and synthetic fibers. As could be observed, fibers with a higher cellulose content (see Table 3.2) generally have

high strength and modulus of elasticity. However, as described before, not only the chemical composition but also physical properties such as MFA and cellulose crystallinity influence the mechanical performance of plant fibers. Even though some of them can have comparable specific properties to artificial ones like glass fiber (Taj et al., 2007, as cited in Djafari Petroudy, 2017), its use is recommended when a high modulus of elasticity is not required (Gholampour & Ozbakkaloglu, 2019). On the other hand, the elongation at break can be better for natural than synthetic fibers (Djafari Petroudy, 2017).

Table 3.3 Properties of several fibers (Gholampour & Ozbakkaloglu, 2019; Vera, 2009; Mori et al., 2018; Yan, Kasal, et al., 2016).

Fiber	Diameter (mm)	Density (g/cm^3)	Tensile strength (MPa)	Elastic modulus (GPa)	Strain (%)
Cotton	-	1.52–1.56	287–800	5.5–12.6	7.0–12.0
Jute	20-200	1.30–1.52	320–860	13.0–60.0	1.0–1.8
Flax	12-600	1.42–1.52	345–2000	27.6–103.0	1.2–3.2
Hemp	25-600	1.47–1.52	270–920	23.5–70.0	1.0–4.0
Kenaf	-	1.44–1.50	195–666	53.0–66.0	1.3–5.5
Ramie	-	1.45–1.55	400–938	61.4–128.0	3.6–3.8
Sisal	8-200	1.33-1.50	363–790	9.4–38.0	2.0–7.0
Coir	10-460	1.15–1.22	95–240	2.2–6.0	15.0–51.4
Pina	-	1.44	413–1627	34.5–82.5	1.6
Abaca	-	1.50	430–760	6.2–20.0	1.0–10.0
Bamboo	-	0.60–1.10	140–800	11.0–32.0	2.5–3.7
Bagasse	-	1.25	222–290	17.0–27.1	1.1
Banana	-	1.35	500	12.0	1.5–9.0
Oil Palm	-	0.70–1.55	80–248	0.5–3.2	17.0–25.0
Curaua	-	1.40	87–1150	11.8–96.0	1.3–4.9
Ichu	55-83	1.47	352-504	23.40-31.30	1.3-1.9
Silk	-	1.30	100–1500	5.0–25.0	15.0–60.0
Feather	-	0.90	100–203	3.0–10.0	6.9
Wool	-	1.30	50–315	2.3–5.0	13.2–35.0
Asbestos	0.15-3	2.60	3000	200.0	2.0-3.0
Glass	9-15	1.90-2.60	2000-3500	60.0-76.0	0.5-4.8
Steel	5-1000	7.80	500-3000	210.0	3.5
Stainless steel	5-100	7.86	2100	160.0	3.0
Carbon PAN, HM	8	1.60-1.70	2500-3000	380.0	0.5-0.7
Carbon PAN, HT	9	1.60-1.70	3450-4000	230.0	1.0-1.5
Carbon Brea, GP	10-13	1.60-1.70	480-790	27.0-35.0	2.0-2.4
Carbon Brea, HP	9-18	1.80-2.15	1500-3100	150.0-480.0	0.5-1.1
Kevlar 29	12	1.44	2900	69.0	4.4
Kevlar 49	10	1.44	2350	133.0	2.5
Nylon	23	1.14	970	5.0	20.0
Polyester	20	1.34-1.39	230-1110	17.0	12.0-150.0
Polyethylene	25-1000	0.92-0.96	75-590	5.0	3.0-80.0

Fiber	Diameter (mm)	Density (g/cm^3)	Tensile strength (MPa)	Elastic modulus (GPa)	Strain (%)
Polypropylene	-	0.90-0.91	140-700	3.5-4.8	15.0

3.2.3 Factors of variability in the properties of plant fibers

Growing conditions such as cultivation, geographical location, weather and other as harvesting stage, fiber obtention, storage, and surface treatments could lead to significant variability in the fiber properties. According to Pickering, Efendy, and Le (2016), the tensile strength decreases after harvesting the plant outside its optimal time, i.e., fully matured plants produce fibers with higher tensile strength than partially matured plants (Ramamoorthy et al., 2015). On the other hand, depending on the fiber type, some methods of extraction allow better mechanical properties, e.g., manually extracted flax fibers have greater strength than mechanically extracted (Pickering et al., 2016). Storage is also important since fibers could be attacked by fungi or bacteria and therefore reduce their quality. Surface treatment methods, either physical or chemical, allow modifying properties such as moisture absorption and morphology, improving the performance when fibers reinforce a matrix. However, unappropriated conditions could weaken the fiber properties, e.g., Saha et al. (2010) has reported a tensile strength decrease after alkali-treatment of jute fibers at high temperatures. Table 3.4 lists some factors that influence the properties of plant fibers.

Table 3.4. Factors affecting the properties of plant fibers (Modified from Yan, Chouw and Jayaraman as reproduced in Yan, Kasal & Huang, 2016).

Factor	Description
Growing conditions	Cultivation, geographical location, fiber location in the plant, growing conditions, e.g., weather.
Harvesting stage	Fiber ripeness influences the cell wall thickness, adhesion between fibers and the surrounding matrix, size and shape of lumen, porosity, and microfibril angle.
Fiber obtention	Mechanical, biological, or chemical method.
Supply stage	Transportation and storage conditions.
Measurement conditions	Tensile speed, initial gauge length, moisture, temperature, cross-section.
Surface treatment	Physical and chemical treatments.

Another reason of variability is the measurement conditions such as gage length and speed test. Silva, Hernández, Caballero & López (2009) studied the mechanical properties of agave fibers extracted from leaves at different plant levels. At lower levels, the tensile strength was around 390 MPa, while at higher levels, it reduced to about 260 MPa. The

length of the specimen and the speed of the test also influenced the mechanical properties. Tensile strength and strain decreased when using a longer length of the specimen, and the modulus of elasticity increased. Although, authors like Indran & Raj (2015) reported a direct relationship between those parameters. On the other hand, tensile strength and modulus of elasticity increased when using a higher test speed, but strain decreased.

3.3 Chemical treatments for natural fibers

The hydrophilic behavior of natural fibers causes interaction issues between the fibers and the matrix. When the geopolymer mortar is fresh, fibers absorb moisture causing them to swell. When the matrix sets, the fibers dry, and their volume decreases. This mechanism weakens the adhesion, also known as interfacial bonding, between the matrix and the reinforcement (Pickering et al., 2016). The inadequate mechanical interaction difficulties the transfer of load and affects the mechanical properties of the composite. Chemical treatments can help overcome these problems since they produce a rougher surface that improves mechanical interaction and promotes a hydrophobic behavior that decreases the moisture absorption capacity (Table 3.5) (Gholampour & Ozbakkaloglu, 2019).

Table 3.5. Chemical treatments for natural fibers.

Chemical treatments	Description
Alkaline	Modifies the cellular structure employing sodium hydroxide solutions.
Acetyl	Insertion of acetyl groups in the cell structure. Removal of amorphous components.
Benzoyl	Replacement of OH groups by benzoyl groups.
Peroxide	Reaction between peroxide groups and OH groups.
Sodium chlorite	Fiber cleaning with sodium chlorite $NaClO_2$ solutions.
Silano	Fibrillar pore coating to promote chemical bonds with the matrix.
Stearic acid	Reaction between carboxyl groups of stearic acid and OH groups. Removal of amorphous components.

3.3.1 Alkaline treatment

Alkaline treatment is a non-cost-effective procedure that uses sodium hydroxide (NaOH) solutions to remove some chemical components. The treatment breaks the NaOH-sensitive structures leading to the dissolution of hydrophilic groups, causing decreased non-cellulosic components (Gholampour & Ozbakkaloglu, 2019). The reactions involved are represented by the following expression (Vasquez et al., 2016)

$$fiber - OH + NaOH \rightarrow fiber - O - Na + H_2O$$

Alkali treatment releases cellulose chains from a state of strain caused by the non-cellulose components. Because rigidity reduces, the fibers can reorient in the direction of load, leading to an increase in the tensile strength (Ray & Sarkar, 2001). The dissolution of amorphous compounds such as hemicellulose and lignin reduces the moisture absorption capacity, and the increase in crystallinity positively influences the tensile strength (Rocha et al., 2015). The dissolution of impurities also creates a rougher surface. The reduction of diameter increases the aspect ratio and specific surface, enhancing the interfacial bonding between the fiber and the matrix (Ray & Sarkar, 2001; Yan, Chouw, et al., 2016).

The treatment can be carried out under variable NaOH concentrations and duration. Depending on the fiber studied, some doses can be inadequate and therefore weaken the fiber. Vasquez et al. (2016) studied the alkali treatment for sweet sorghum fibers. At higher concentrations, the tensile strength decreased due to the removal of non-cellulosic in excess. Juarez (2002) suggests that high alkalinity changes the cellulose structure, leading to new compounds. According to El Oudiani et al. (2012), high NaOH concentrations decompose glucose, the principal constituent of cellulose, and stimulates the transition from cellulose I to cellulose II. The problem is that the crystallinity, a property related to the mechanical strength of the fiber, decreases in cellulose II. The transition between cellulose structures could start since 2% and be more pronounced between 10% and 15% NaOH concentration.

The treatment can be carried out under variable conditions of pressure and temperature. High temperatures have a negative impact due to the degradation of the cell structure. Saha et al. (2010) studied the alkali treatment for jute fibers at room, elevated temperatures, and under pressure. At room temperature (30°C±2°C), the suitable condition was 4% NaOH concentration over 0.5 hr. The tensile strength increased by 50%, and the elongation by 54%. At elevated temperatures (90°C±2°C), 1% NaOH concentration over 0.5 hr increased the tensile strength by 40% and the elongation by 23%. Under pressure and elevated temperature (103±2 kPa and 125±2°C), 0.5% NaOH concentration over 0.5 hr increased the tensile strength by 65%, although the strain was reduced by 38%.

3.4 Cracking mechanisms: Stress transfer and fiber bridging

Even before loads are applied to the composite, there are already microcracks caused by shrinkage, thermal deformations, and internal constraints. When carrying loads, the microcracks grow and propagate until the composite reaches the peak load, then the propagation of cracks is unstable and triggers the appearance of macrocracks (Löfgren, 2005). Fibers act when the first crack appears (Concrete Technology Weblog, 2008) by the development of bridging mechanisms that help reduce the crack width (Figure 3.5). However, studies have shown that fiber reinforcement does not considerably increase the tensile strength of unreinforced matrices mainly to the low tensile strain capacity of the matrix and due to the increase of porosity (Löfgren, 2005). Fiber reinforcement allows the composite to increase its fracture toughness, that is, the area under the stress-strain curve due to the absorption of large amounts of energy that shifts the failure mode from brittle to ductile (Concrete Technology Weblog, 2008). The fiber pull-out is the preferred mechanism between the fiber failure modes because it requires higher energy to overcome friction forces (Noushini et al., 2018).

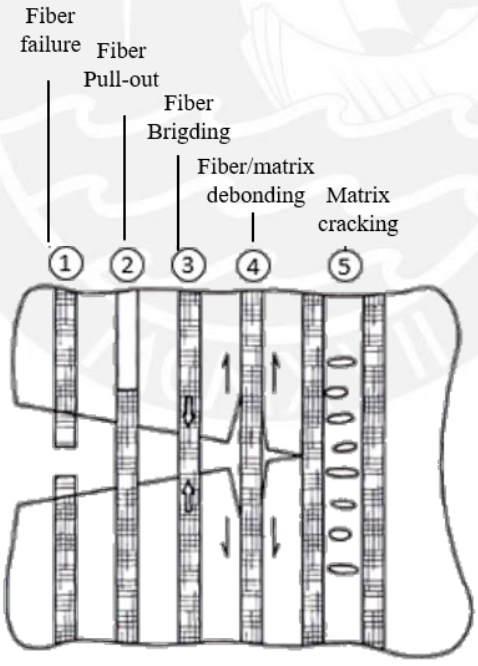

Figure 3.5. Fiber fracture mechanisms in reinforced composites (Zollo, 1997).

3.4.1 Fiber content in cementitious composites

A suitable fiber content prevents fiber agglomeration and reduces the air bubbles entrapped into the matrix. Moreover, it does not reduce workability and controls the moisture absorbed from the matrix (Pickering et al., 2016). Hence, it is an important parameter to control the mechanical properties of the composite. Fiber concentrations, in volume, for cement composites can be divided into three categories: (i) low between 0.1% to 1%, (ii) moderate between 1% to 3%, and (iii) high between 3% to 12%. Low ranges are recommended for batch mixing, while higher concentrations require special techniques for the mixture (Zollo, 1997). Figure 3.6 shows the typical fiber concentration used by type and volume percent of the matrix.

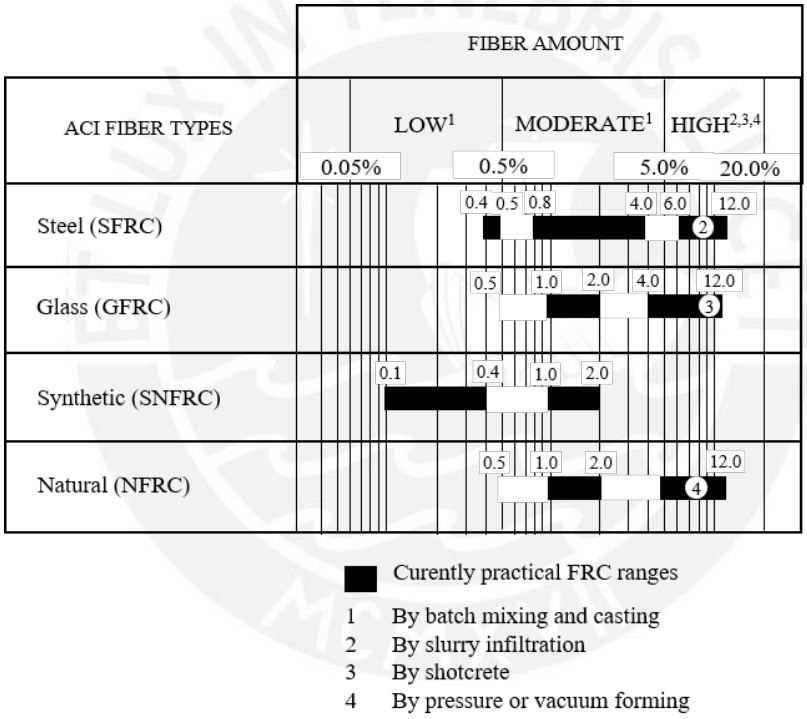

Figure 3.6. Typical fiber concentrations by type and volume percent of the matrix (Zollo, 1997).

CHAPTER 4. Fiber obtention, optimization of alkaline treatment, and characterization of *Agave americana* fiber

Abstract. This chapter develops the obtention, the process of alkaline treatment, and characterization of *Agave americana* fiber. The fibers were obtained by beating and boiling the leaves and then treated with 1%, 5%, and 20% NaOH concentrations over 0.5 hr, 1 hr, and 3 hr. They were tested according to the ASTM C1557 to determine the tensile strength and observed by scanning electron microscopy (SEM) to understand the influence of the treatment on the fiber surface. Generally, treated fibers obtained higher tensile strength and strain, being 1% NaOH concentration over 1 hr the optimum condition, which led to an increase of 87% in the tensile strength and of 217% in the strain. The modulus of elasticity decreased by 50% at this condition. Further, the SEM analysis identified 20% NaOH over 3 hr as a potentially aggressive treatment for the agave fibers.

4.1 Introduction

Agave americana, also known as cabuya or maguey, is a succulent plant with fleshy leaves of up to 2 m and sharp tips (Global Invasive Species Database, 2020). This species is native to Central America and has a wide geographical distribution due to its weather resistance. Their rigid leaves are constituted of fibers with high hydrophilicity, low density, and high tenacity and deformation capacity (Bezazi, Belaadi, Bourchak, Scarpa & Boba, 2014). Agave leaves are composed of 68% to 80 % cellulose, 15% hemicellulose, 5% to17% lignin, and 0.26% waxes (Hulle, Kadole & Katkar, 2015).

The alkaline method is one of the simplest chemical treatments for natural fibers. It consists of soaking them into sodium hydroxide solutions to remove the non-cellulosic components that constitute the natural matrix. This mechanism allows the cellulose fibrils to be reoriented in the load direction, enhancing the fiber strength. The reduction of non-cellulosic compounds promotes a hydrophilic character and increases the fiber roughness for better interfacial bonding between the matrix and the fiber.

Bezazi et al. (2014) produced agave fibers by (i) burying the leaves under 0.3 m to 0.4 m depth for three months and (ii) by retting the leaves for 10 to 13 days. The fibers had tensile strength between 128 MPa to155 MPa, strains between 26% to 52 %, and modulus of elasticity between 1.3 GPa and 2.1 GPa. Kestur et al. (2013) extracted fibers by grinding cooked agave stem that was the bagasse from tequila production. The fiber tensile strength was between 50 MPa to 58 MPa, strains between 11% to 15 %, and modulus of elasticity between 2.6 GPa to 2.9 GPa. Silva et al. (2009) produced fibers by the retting method of *Angustiola haw* agave leaves and determined fiber tensile strengths between 163 MPa to 550 MPa, strains between 1.1% to 2.9 %, and modulus of elasticity between 11 GPa to 24 GPa.

Chemical treatments have also been studied in *Agave americana* fibers. Bessadok, Marais, Roudesli, Lixon & Métyer (2008) produced fibers by immersing the agave leaves in pectinase solution for 12 hr. Then treated the fibers with maleic anhydride, acetylation, acrylic acid, and styrene to modify the water absorption capacity. The untreated fibers obtained tensile strengths between 65 MPa to 154 MPa, strain between 13.6 %to 22.3%, and modulus of elasticity between 1.3 GPa to 2.9 GPa. The styrene and the maleic anhydride treatments effectively reduced the water absorption capacity and increased the fiber

strength. El Oudiani et al. (2012) extracted agave fibers through hydrolysis and treated the fibers with sodium hydroxide at 30°C for 1 hr. The study used NaOH concentrations of 1, 2, 5, 10, 15, 20 and 30%. Low NaOH concentrations less than 2% lead to increments of the strength, but higher concentrations weaken the fibers producing results even below untreated fibers. Others, however, have used high concentrations of sodium hydroxide, obtaining favorable results. Gassan and Bledzki (1999, as cited in Saha et al., 2010) used a 28% NaOH concentration and reported a 120% increase in tensile strength for jute fibers.

This chapter studies the optimization of NaOH concentration and duration of alkaline treatment for *Agave americana* fibers. The natural fibers were dipped in 1%, 5%, and 20% NaOH concentration for 0.5 hr, 1 hr, and 3 hr at room temperature and tested following the ASTM C1557 (ASTM International, 2014) to determine the tensile strength. Their morphology was analyzed by scanning electron microscopy (SEM) to understand the treatment effect on the fiber surface. This chapter aims to verify whether the alkaline treatment improves the tensile strength and which condition enhances it efficiently.

4.2 Materials and methods

Figure 4.1 illustrates the steps considered for the characterization of the *Agave americana* fibers. As mentioned, the fibers were extracted through heating and boiling the leaves (Section 4.2.1) and treated with sodium hydroxide at different concentrations and times (Section 4.2.2). The mechanical characterization aimed to obtain the tensile strength, strain, and modulus of elasticity for the control and alkali-treated fibers (Section 4.2.3). Further, SEM analysis was performed to observe the effect of the alkaline in the fiber surface (Section 4.2.3). The characterization aims to suggest an optimum alkaline treatment condition.

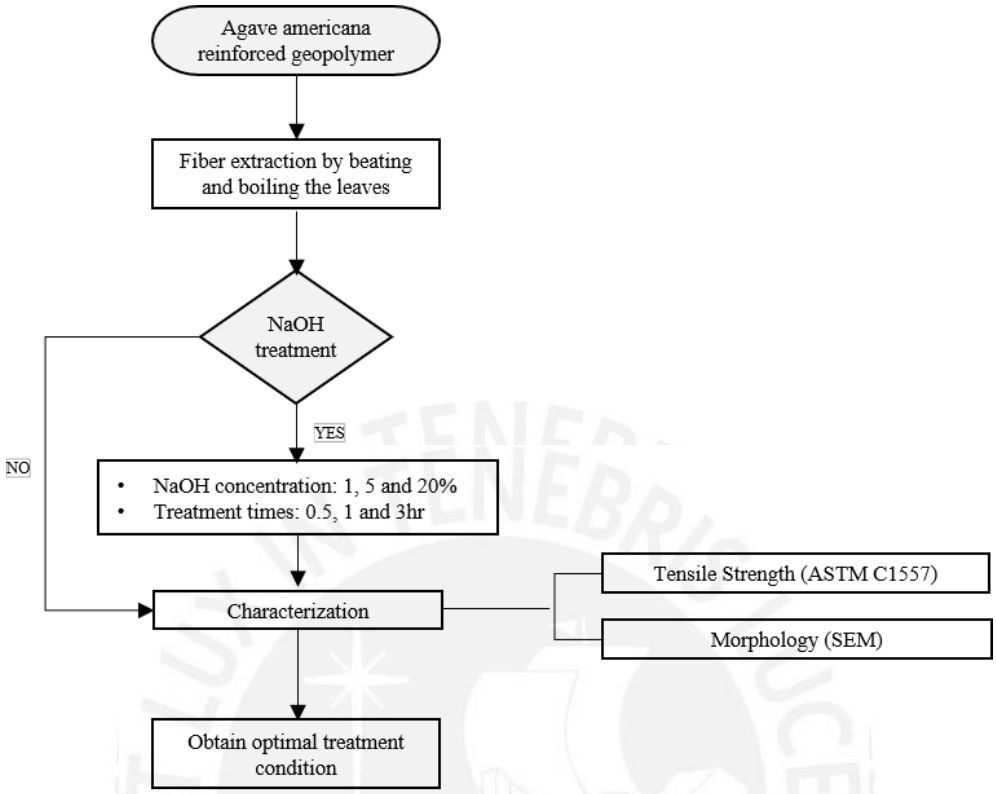

Figure 4.1 Flowchart of the characterization of natural and alkali-treated *Agave americana* fiber

4.2.1 Fiber obtention

Figure 4.2a shows the process for the obtention of the *Agave americana* fibers. The leaves were obtained from the agave plant shown in Figure 4.2b. First, they were beaten with wooden rollers and submerged in boiling water (Figure 4.2c), crushed with the rollers to extract the pulp (Figure 4.2d) and separated with a metal brush (Figure 4.2e). Once separated, the fibers were rinsed with boiling water, which was necessary to quit the sticky pulp, and left a couple of days in the open air to dry (Figure 4.2f). Finally, they were stored in aluminum bags to conserve their moisture until the preparation of specimens.

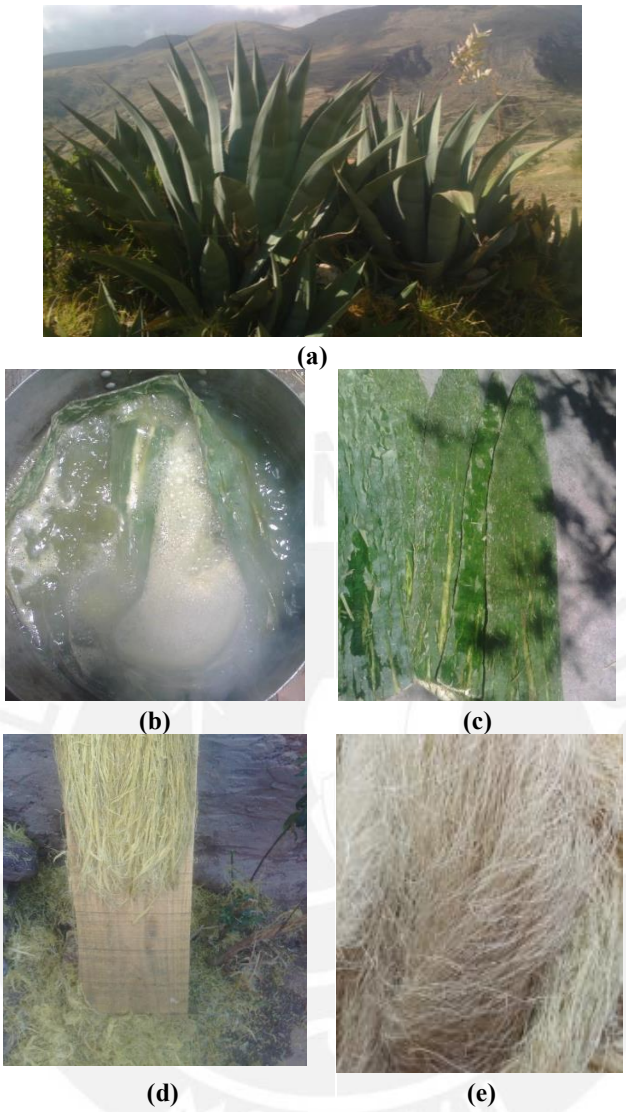

Figure 4.2 Process for the obtention of the *Agave americana* fiber: (a) agave plant at natural habitat at the region of Junin (Peru), (b) leaves submerged to boiling water for two hours, (c) leaves after the process of crushing to extract the pulp, (d) fibers brushed to clean the pulp residues and (e) dry fibers after couples of days of being washed with boiling water.

4.2.2 Alkaline treatment of *Agave americana* fibers

Sodium hydroxide pellets of 99% purity were used for the alkaline treatment (Figure 4.3a). The agave fibers were soaked in 1%, 5%, and 20% NaOH solutions at room temperature over 0.5 hr, 1 hr, and 3 hr (Figure 4.3b). The ratio between the fiber weight to the alkaline solution was 1:50 for all the conditions. After the treatment, the fibers were neutralized with 1 % acetic acid solution over 10 min to remove alkali traces (Figure 4.3c) and rinsed with fresh water (Figure 4.3d). Finally, the agave fibers were placed in an oven (Model BD 56,

BINDER, Germany) at 65°C over 24 hours and kept in sealed bags until the tensile strength test.

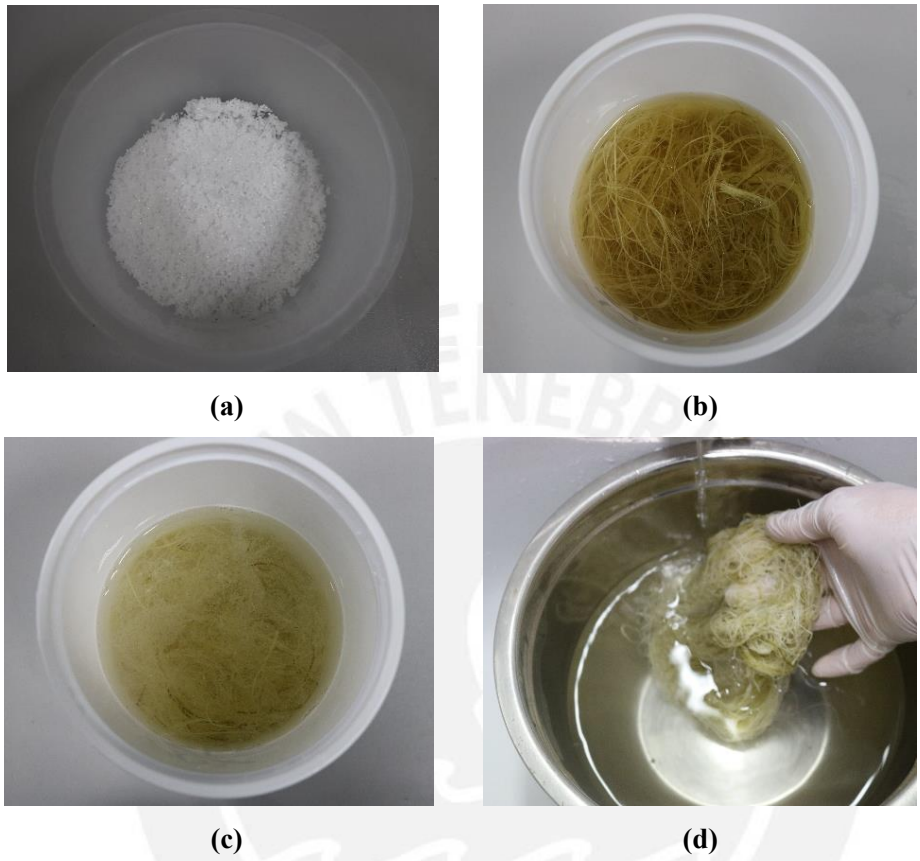

Figure 4.3 Alkaline treatment for *Agave americana* fibers: (a) sodium hydroxide (NaOH) pellets, (b) fibers during alkaline treatment, (c) neutralization with 1% acetic acid after soaking in alkaline solution and, (d) rinsed with fresh water after neutralization.

4.2.3 Characterization

- **Tensile strength of *Agave americana* fibers**

The tensile strength test was conducted on alkali-treated and control fibers in accordance with the ASTM C1557 using an electromechanical machine (Exceed E42, MTS, USA) with a load capacity of 5 kN (Figure 4.4a) and standard grips. Mounting tabs (Figure 4.4b) were used to prevent the slippage of the fibers from the grips. Super Glue (CHEMMER, Peru) was used to adhere the fibers to the cardboards. Before the test, the mounting tabs were cut, as shown in Figure 4.4c. The test speed was 10 mm/min.

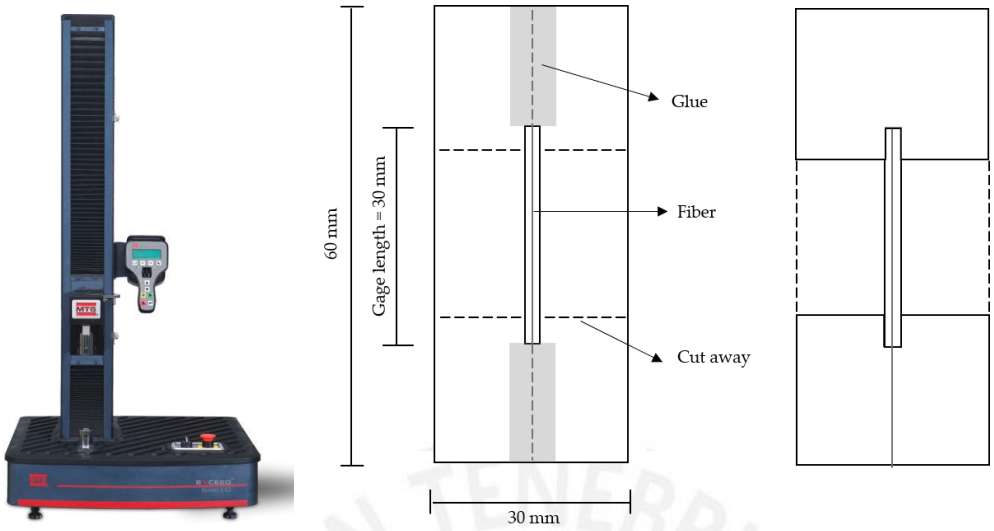

Figure 4.4 Preparation of specimens for the tensile strength test: (a) electromechanical machine (Exceed E42, MTS, USA) (Direct Industry, n.d.-a), (a) fiber setup on the mounting tab, and (b) detail of the mounting tab cut before the test.

For each condition, at least ten specimens of 30 mm gage length were tested. Figure 4.5a shows a specimen after the test, and those who broke near the gripping area were discarded, as shown in Figure 4.5b. The diameter of the fibers was determined in the vicinity of the failure zone, as suggested in the standard, using an optical microscope (DM750, Leica, Germany) (Figure 4.6).

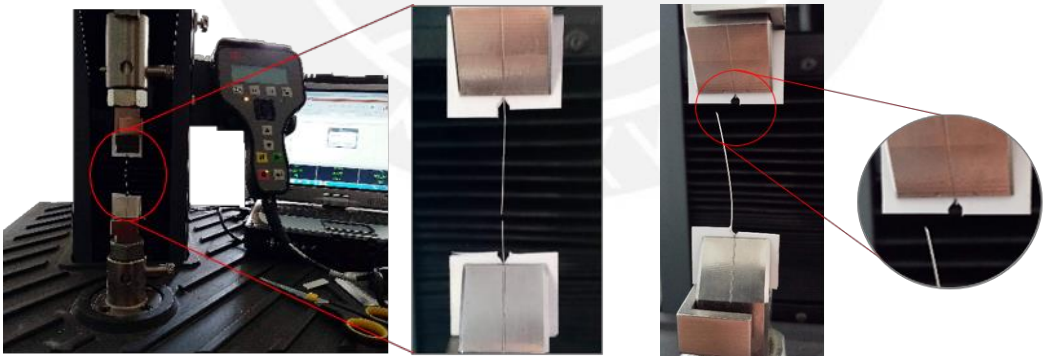

Figure 4.5 Tensile strength specimens after the test: (a) detail of fiber failure and (b) invalid specimen that broke near the gripping area.

(a) **(b)**

Figure 4.6 Diameter measurement in the vicinity of the failure zone in accordance with the ASTM C1557 (ASTM International, 2014): (a) optical microscope (DM750, Leica, Germany) and (b) detail of the specimen.

The mechanical properties were calculated using the equations listed below, considering a circular cross-section. The modulus of elasticity was determined from the linear zone of the tensile strength-strain curve (Young's Modulus).

$$\sigma = \frac{F}{A}$$

where: σ is the tensile strength (Pa), F is the force at failure (N), and A is the cross-section in the failure zone normal to the fiber axis (m^2).

$$\varepsilon = \frac{\Delta l}{lo}$$

where: e is the elongation of test length, ΔL is the total elongation (m), and lo is the test length (m).

- **Morphology of agave fiber surface**

The morphology of the fibers was observed using scanning electron microscope SEM (FEI-Quanta 650, Thermo Fisher Scientific, USA) for the control fibers, highest and lowest conditions of alkaline treatment: 1 % NaOH concentration over 0.5 hr and 20% NaOH over 3 hr. Before the analysis, the specimens were covered with a thin layer of gold and observed at SEM using 10 kV and 500x and 2000x magnifications.

4.2.4 Box plots

The results were plotted in a boxplot which bases data distribution on five representative values: the minimum, first quartile (Q1), median (Q2), third quartile (Q3), and the

maximum. It is possible to identify outliers or extreme values in a boxplot, which do not influence quartiles, unlike the mean and standard deviation (Krzywinski & Altman, 2014). The size of the box represents the variability around the median (Williamson, D F et al., 1989). Figure 4.7 shows a typical boxplot. Mean values were also included for illustration.

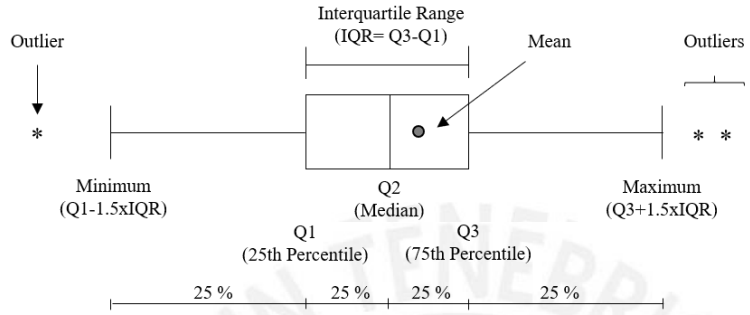

Figure 4.7 Parts of a box plot.

4.3 Results and discussion

4.3.1 Tensile strength of Agave americana fibers

The alkaline treatment removes non-cellulosic components to allow cellulose fibrils to reorient in the direction of load, increasing the fiber strength. But, a very low concentration of alkali may be insufficient to remove impurities (Thirumalaisamy & Pavayee Subramani, 2018), and when the concentration is too high, cellulose fibrils lose their parallel orientation; thus, affecting the fiber strength (El Oudiani et al., 2012). In this study, no chemical or physical analyses were carried out to identify chemical composition changes or crystallization degrees. According to El Oudiani et al., (2012), the degree of crystallinity in *Agave americana* fibers (extracted by hydrolysis) may start to decrease at 2% NaOH concentration and at 15% of concentration the remaining cellulose type is cellulose II, characterized for its lower crystallinity. A similar conclusion was obtained by Chen et al., (2017) in studying the alkali treatment for individual bamboo fibers.

The box plot of Figure 4.8 shows the results of the tensile strength tests. A high variability was observed, typical when working with natural fibers as reported in the literature(Kestur G. et al., 2013). A general tendency to improve the tensile strength after the treatment is appreciated, unlike other fiber studies in which the treatment had a negative effect (Machaka et al., 2014). For the control condition, a non-unusual minimum of 40 MPa and a maximum of 275 MPa were obtained, with at least 50% of the observed values greater than 155 MPa. The conditions 1% 1 hr and 5% 1 hr had higher median values, after which the strengths

tended to decrease. The 1% 1hr condition had a non-unusual minimum of 155 MPa, a value greater than 50% of the lowest control data. The condition presented a median of 290 MPa, representing an increase of 87% in respect of the control fibers. Besides, it has less variability than other conditions with a high median, like 5% 1 hr, which indicates that 1% 1 hr data are more consistent. This condition also required the least resources to improve the tensile strength effectively.

The results showed a similar trend to that obtained by Saha et al. (Saha et al., 2010) when performing alkaline treatment on jute fibers (commercial type). NaOH concentrations between 0.5% to 18% were evaluated during 0.5 hr to 24 hr, finding an optimal condition at 4% 0.5 hr with improvements of up to 50% in the fiber tensile strength. Their results also show appreciable improvements when using 1% 1 hr and 4% 1hr with increments of around 45%. Thirumalaisamy and Pavayee Subramani (Thirumalaisamy & Pavayee Subramani, 2018) also used alkaline treatment for Agave Angustifolia Marginata fiber (extraction by decortication) under 2%, 5%, 10% and 15% NaOH concentrations of for 1 hr,2 hr, 4 hr, 6 hr, and 8 hr. The optimal condition was 5% 1 hr, after which the fiber strength started to decrease.

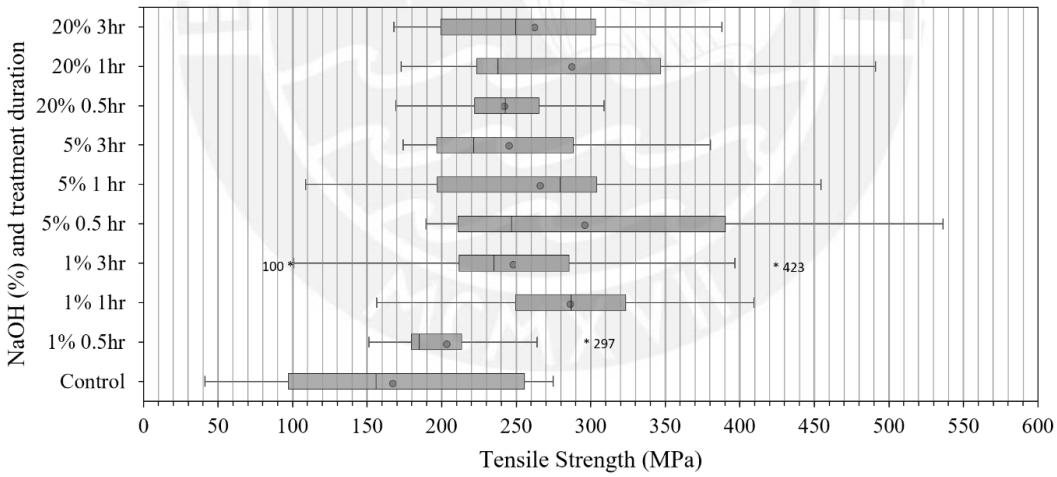

Figure 4.8 Box plot for the tensile strength results for natural and alkali-treated agave fibers.

When comparing the strains (Figure 4.9), it can be observed that the alkaline treatment gave the agave fibers greater deformation capacity. It was possible because the treatment removes amorphous components, e.g., lignin (Chaabouni et al., 2006), which provides plant fibers a rigid behavior, letting them behave more flexibly (Rocha et al., 2015). The optimal condition of alkali treatment, 1% 1hr, obtained a median of 0.38 mm, representing an

increase of 217% in respect to that of the control fibers, 0.12 mm. It can be observed that after 1% 1 hr, the elongation at break tends to decrease. This trend differs from the study of Chen et al. (Chen et al., 2017), who found improvements in the elongation at break of individual bamboo fibers when using NaOH concentrations higher than 10%, with the maximum increase of 232% corresponding to 15% NaOH concentration. Theoretically, the decrease in cellulose crystallinity will increase the elongation at the break since cellulose fibrils will be able to twist (Djafari Petroudy, 2017). However, individual fibers generally have lower properties due to the slippage effect of fibers (Célino et al., 2014) and because they contain greater defects.

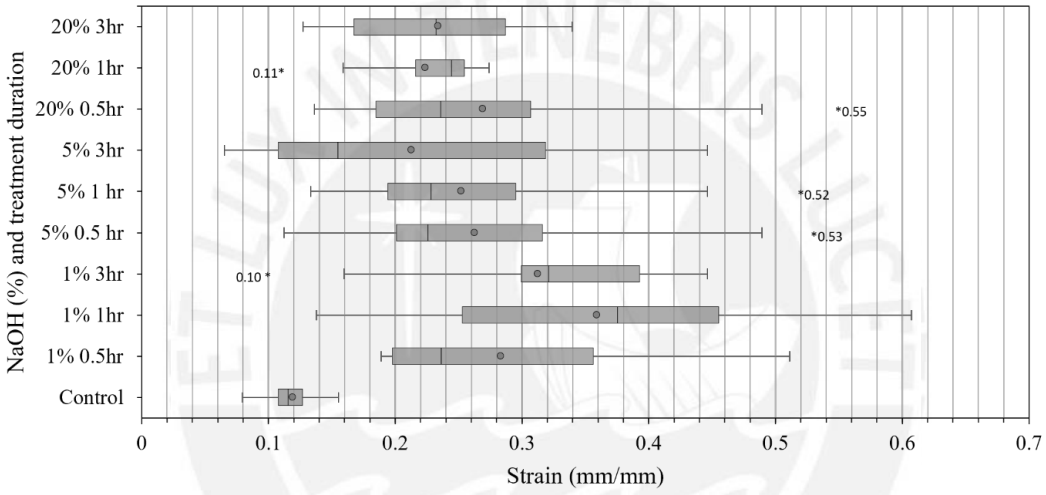

Figure 4.9 Box plot for the strain results for natural and alkali-treated agave fibers.

The modulus of elasticity was obtained from the linear region of the curves presented in Figure 4.10 and Figure 4.11 for the control and alkali-treated agave fibers. Figure 4.12 shows the box plots for the E values. When comparing the medians, the control fibers obtained 0.78 GPa and the treated condition 0.40 GPa, representing a decrease in the modulus of elasticity by about 50%.

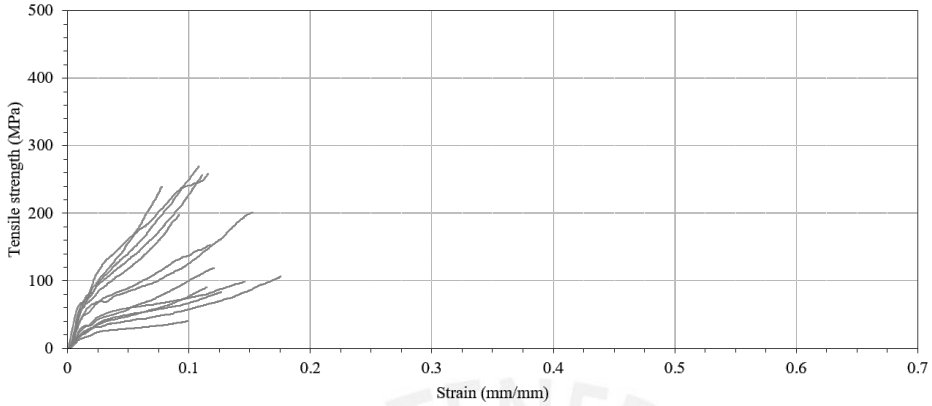

Figure 4.10 Tensile strength-strain curves for the control fibers.

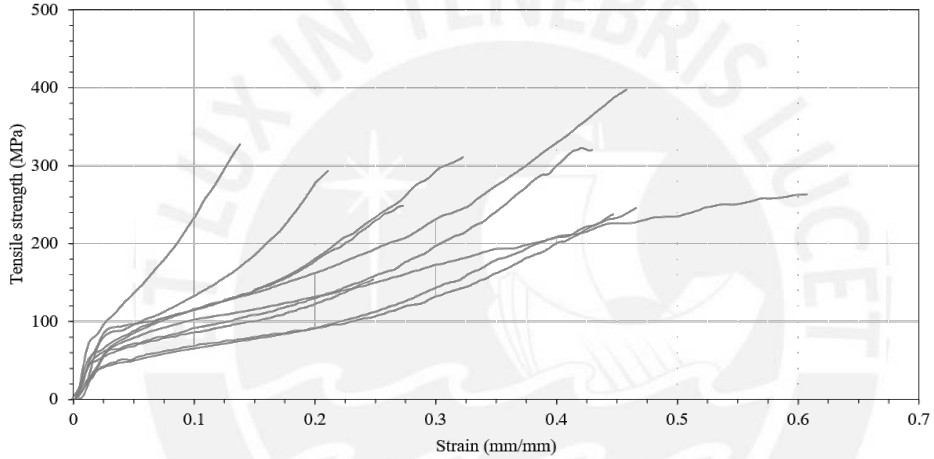

Figure 4.11 Tensile strength-strain curves for the alkali-treated fibers at 1% NaOH concentration over 1 hr.

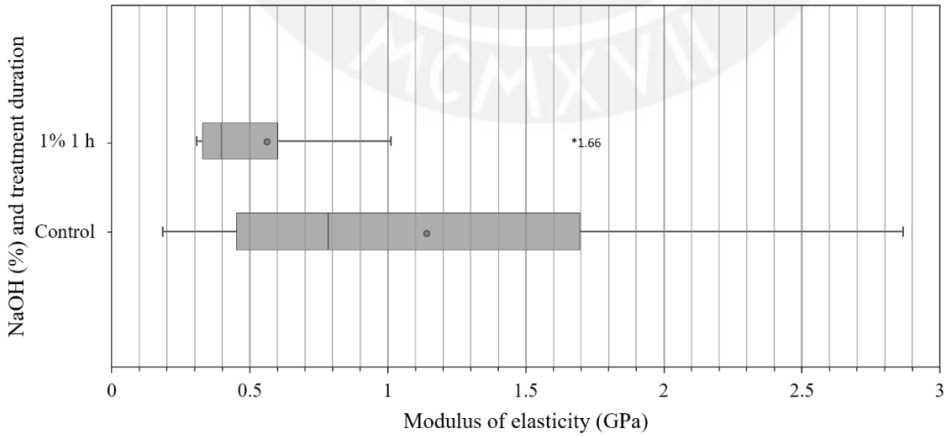

Figure 4.12 Modulus of elasticity for the control and alkali-treated fibers at 1% NaOH concentration over 1 hr.

4.3.2 Morphology

Figure 4.13 shows the SEM images for the control scenario (Figure 4.13[a] and [b]), alkali-treated fibers at 1% NaOH concentration over 0.5 hr (Figure 4.13[c] and[d]) and 20% NaOH concentration over 3 hr (Figure 4.13[e] and [f]). It could be observed a rough and heterogeneous surface throughout the fiber length for all the specimens compared to synthetic fibers, as mentioned in Chapter 3. Alkali-treated fibers showed retracted surfaces caused by dehydration due to the process. The fibers treated with the highest NaOH concentration: 20% NaOH over 3 hr showed an apparent decomposition of the structure, which would suggest that such a high concentration of NaOH and duration could be aggressive and weaken the agave fibers.

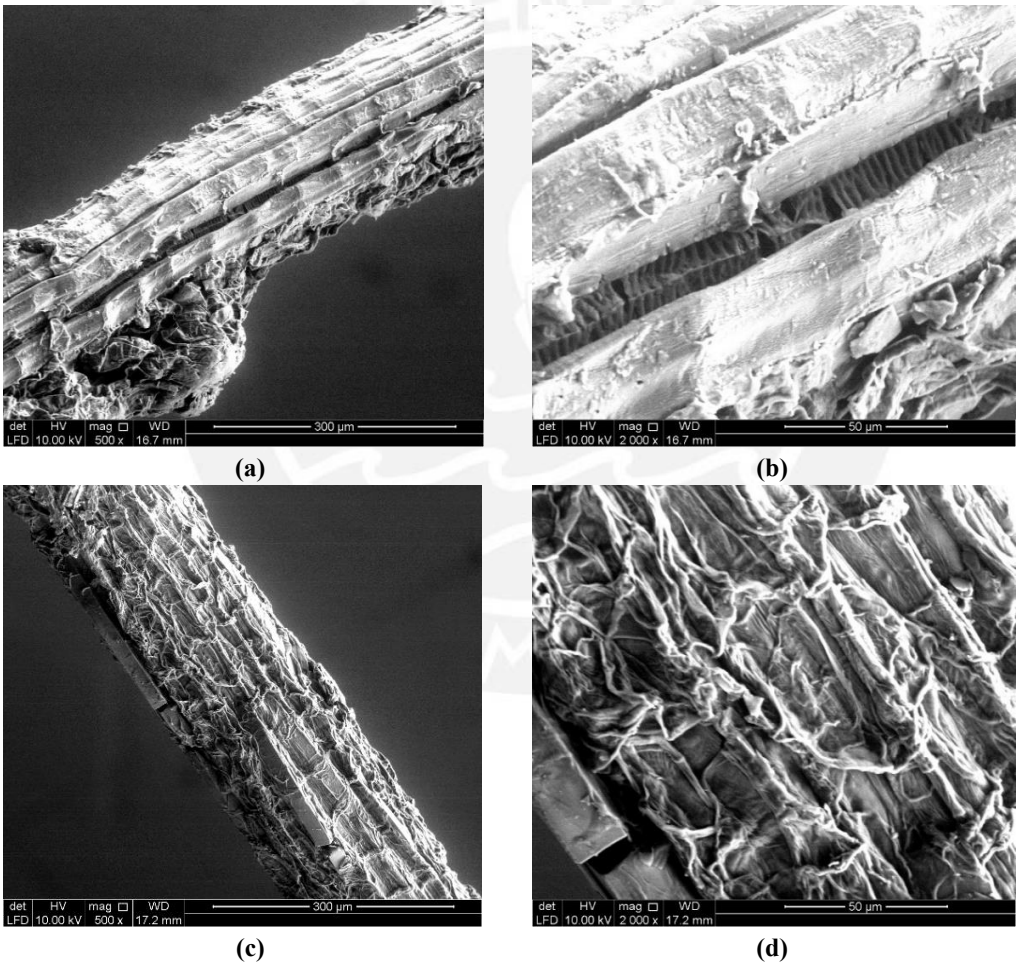

(a) **(b)**

(c) **(d)**

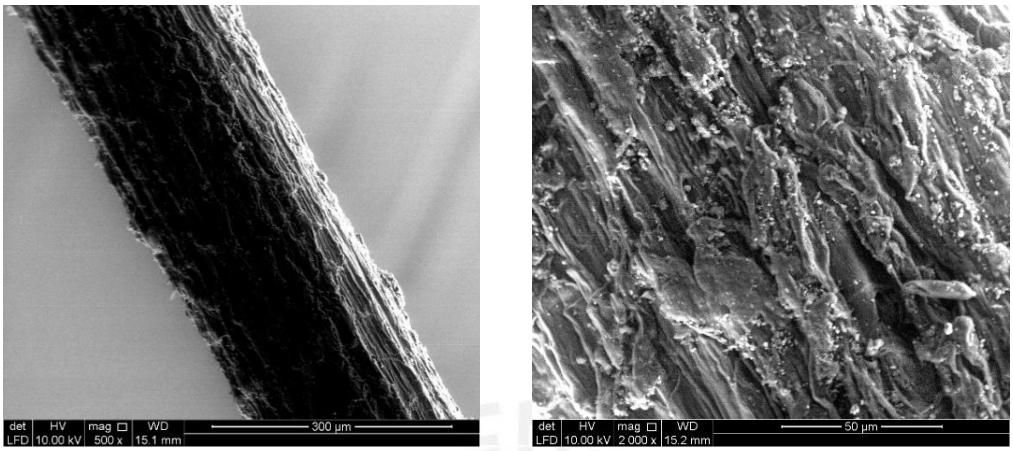

(e) **(f)**

Figure 4.13 Scanning electron microscopy (SEM) images for Agave americana fibers: (a) control fiber, (b) detail of control fiber from (a); (c) alkali-treated fiber at 1% NaOH concentration over 0.5 hr, (d) detail from (c); (e) alkali-treated fiber at 20 % NaOH concentration over 3 hr, and (f) detail from (e).

CHAPTER 5. Optimization of fiber content and characterization of agave fiber-reinforced fly ash-based geopolymer

Abstract. This chapter studies the influence of *Agave americana* fiber on the mechanical behavior of fly ash-based geopolymers. The fibers were treated at 1% NaOH concentration for 1 hr and added to the mixture at 0.5%, 0.75%, and 1% by weight of fly ash. They were tested to determine the compressive, flexural, and splitting tensile strength at 7 days of age. The results suggest that the compressive strength may not be significantly affected by the addition of fibers reporting an increase of up to 12% for the compressive strength and 13% for the modulus of elasticity in respect to the control specimens. On the other hand, the flexural strength did not improve with the fiber addition and decreased for the evaluated conditions of up to 22%. The fiber length may cause this issue, as reported in some studies. Further, results suggest that the splitting tensile strength tends to increase with the addition of fiber. The maximum increase was registered with the addition of 1% fiber content by 36%. Finally, the SEM images identified the pull-out, debonding, and breakage as the fiber failure modes, which may have delayed the geopolymer fracture and changed its failure mode from brittle to ductile.

5.1 Introduction

In order to improve their brittle behavior, geopolymers are reinforced with fibers. The fibers allow adequate distribution of the loads enabling multiple cracking and increasing the composite ductility. The fibers act when the first macrocrack appears, and because they can develop bridging mechanisms, it is possible to delay the failure of the composite (Löfgren, 2005). However, to efficiently reinforce the material, a suitable fiber content must be used to avoid the agglomeration of the reinforcement in the matrix and consequently the inclusion of air, which are the primary deficiencies when using fibers.

Kroehong, Jaturapitakkul, Pothisiri & Chindaprasirt (2018) investigated the effect of alkali-treated (2%NaOH for 24 hours) oil palm fibers (25 mm length) on fly ash-based geopolymer at 1%, 2%, and 3% fiber content at seven and 28 days of age. The compressive strength results showed a tendency to decrease as the fiber content increased. At 7 days of age, the control matrix had 28.1 MPa, and a maximum reduction in strength was obtained at 3% fiber content, probably caused by the increase of porosity due to the addition of fibers. The flexural strength for the unreinforced geopolymer was 2.56 MPa at 28 days of age and increased up to 2% by 59% reinforced samples. Chen et al. (2014) investigated the reinforcement of fly ash-based geopolymer with alkali-treated (2M NaOH over 12 hours) sweet sorghum fiber (<50 mm length) at 1%, 2%, and 3% fiber content. Compressive, flexural, and splitting tensile strength were tested at 7 days of age. For the compressive strength, a similar trend to that of Kroehong et al. (2018) was observed because the strength decreased as the fiber content increased. The compressive strength for the unreinforced specimens was 27.7 MPa and decreased to 20.4 MPa at 3% fiber content. For the flexural and splitting tensile test, the strength increased up to 2% fiber content. Alomayri & Low (2013) investigated the influence of cotton fiber (10 mm length) at 0.3%, 0.5%, 0.7%, and 1 % fiber content to reinforce fly ash-based geopolymers. The compressive strength of geopolymers at 28 days of age increased up to 0.5% fiber content. The highest addition of fibers, such as 0.7% and 1 %, reduced workability and required the use of water. Moreover, their geopolymers had poor fiber dispersion, which led to greater inclusion of voids. Yan, Chouw, et al. (2016) investigated the effect of 1% fiber content alkali-treated (5% NaOH at 20°C for 30 minutes) coir fibers (50 mm length) on the compression and flexural strength of OPC at 28 days of age. The reinforced specimens showed better mechanical performance than the unreinforced ones. For the compressive strength, a value of 22.4 MPa was obtained

for control specimens and increased by 7% after reinforcement. It was also possible to verify an enhancement for compression strain from 0.2% for unreinforced specimens to 0.32% for the reinforced ones. However, the modulus of elasticity decreased by 2% for 28.6 GPa for specimens without reinforcement. On the other hand, the flexural strength increased by 21% with respect to 9.8 MPa for geopolymers without reinforcement.

This chapter studies the optimization of alkali-treated *Agave americana* fiber content for the reinforcement of fly ash-based geopolymer. Agave fibers of 10 mm length were treated at the optimum alkaline condition recommended in Chapter 4 (1% NaOH over 1 hour) and added at 0.5%, 0.75%, and 1% doses. The geopolymers were characterized by compressive, flexural, and splitting tensile strength tests at 7 days of age. The microstructure of the geopolymers was analyzed by scanning electron microscopy (SEM) to identify the fiber bridging mechanisms that could lead to an increase in mechanical performance. This chapter aims to verify whether the mechanical properties increase by adding agave fibers and which fiber content enhances them efficiently.

5.2 Materials and methods

Figure 5.1 illustrates the steps considered for the characterization of the control (unreinforced) and alkali-treated *Agave americana* fiber reinforced fly ash-based geopolymer. The optimum condition of alkaline treatment determined in Chapter 4 was used to treat the fibers. The mechanical characterization included compressive, flexural, and splitting tensile strength tests. Also, the morphology was analyzed to observe the fiber failure modes. This chapter aims to determine the influence of the fiber content on the mechanical properties of fly ash-based geopolymers.

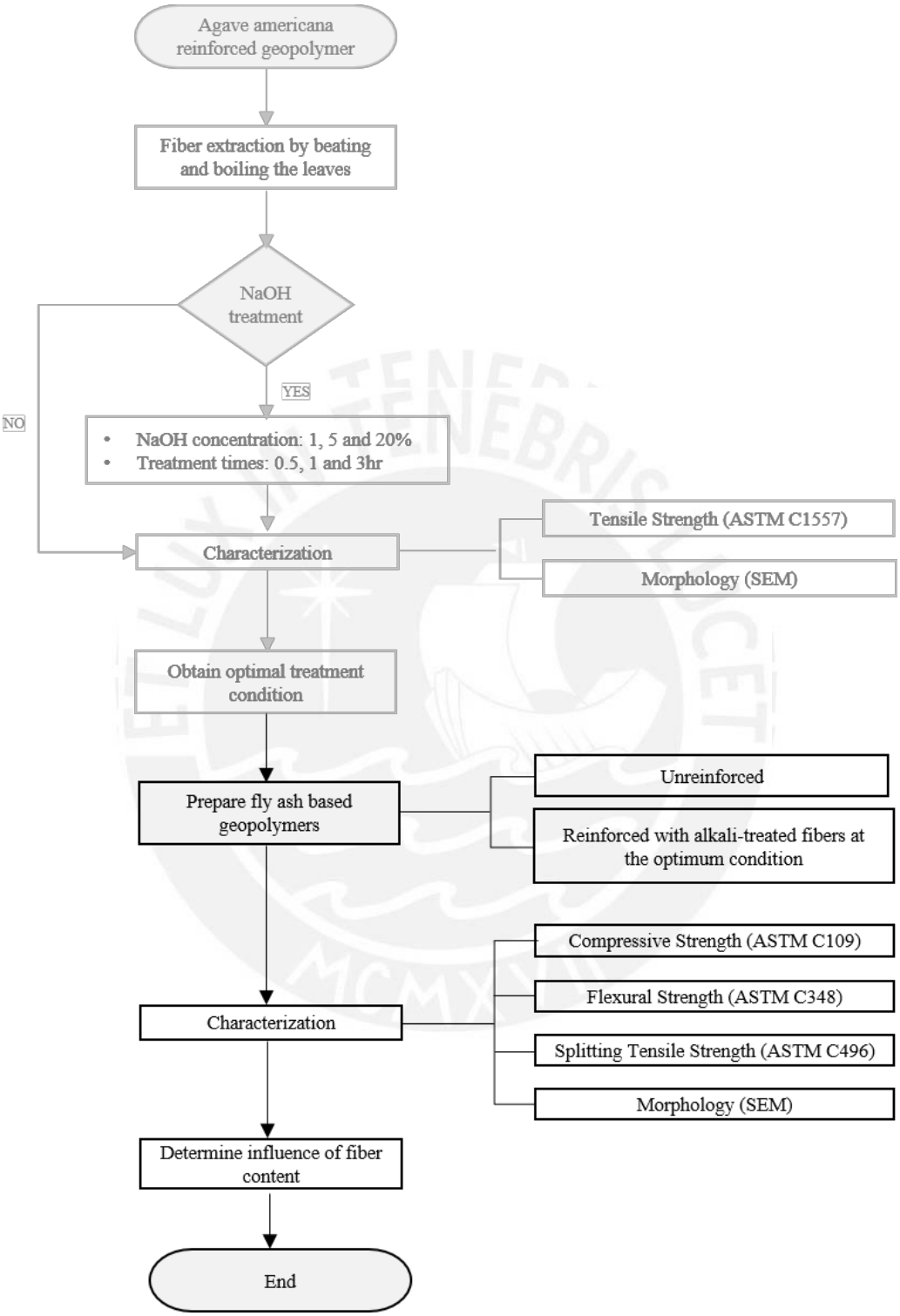

Figure 5.1 Flowchart of the characterization of control and alkali-treated *Agave americana* fiber reinforced fly ash-based geopolymer.

5.2.1 Fly ash

A low-calcium, Class F, donated by the University of North Carolina at Charlotte was used as the raw material. The chemical composition was analyzed by energy-dispersive X-ray spectrometer (SEM-EDX) (Figure 5.2, Table 5.1) and X-ray fluorescence (XRF) (Table 5.2). From the SEM-EDX method, Si (16%), Al (11%), O (44%), and Fe (4%) were identified as the main elements, and the presence of others such as Na, Mg, S, K, Ca, and heavy metal Ti with l% or less of the composition. X-ray fluorescence (XRF) method indicates that about 80% of the mass is constituted by silicon and aluminum oxides with a Si:Al ratio of 2.

Studies reported that a high percentage of loss on ignition (LOI) negatively impacts the compressive strength of geopolymers due to a reduced chemical activity of the fly ash and the required use of water (Sagawa et al., 2015; Wattimena & Hardjito, 2017). Table 5.2 shows that the fly ash has a LOI=2.79, a value lower than 6%, as recommended by the ASTM C618 (ASTM International, 2019). On the other hand, the morphology was analyzed using a scanning electron microscope SEM (FEI-Quanta 650, Thermo Fisher Scientific, USA) (Figure 5.3). It was possible to identify a wide range of sizes and typical morphologies from spherical to irregular and smooth to rough particles.

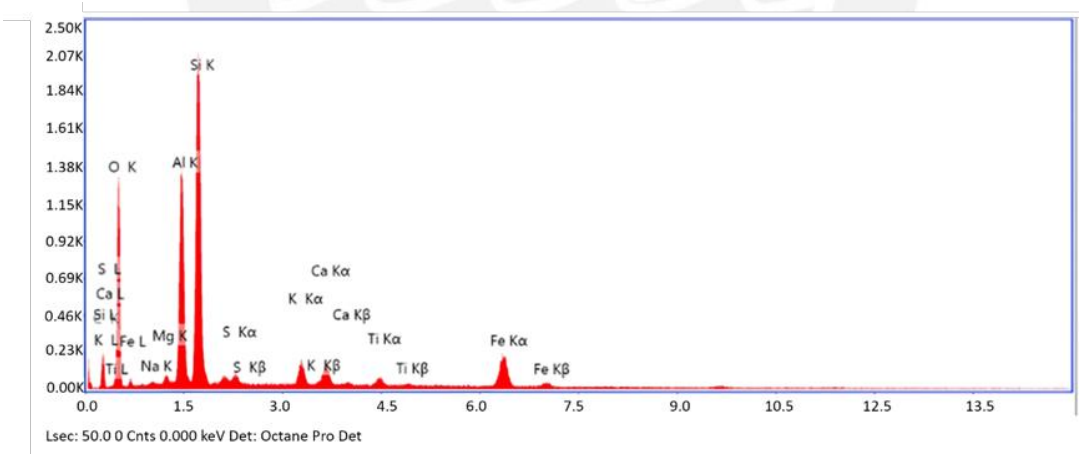

Figure 5.2 SEM-EDX spectra of fly ash particles.

Table 5.1 Chemical composition of fly ash particles determined by SEM-EDX.

Element	C K	O K	Na K	Mg k	Al K	Si K	S K	K K	Ca K	Ti K	Fe K
(%)	19.83	44.21	0.98	0.67	10.55	15.85	1.14	1.13	1.26	0.58	3.79

Table 5.2 Chemical composition of fly ash determined by X-ray fluorescence (XRF).

Component	SiO_2	Al_2O_3	Fe_2O_3	K_2O	CaO	TiO_2	MgO	Na_2O	LOI	Others
(%)	54.71	27.45	9.98	2.26	1.65	1.29	0.92	0.29	2.79	0.27

Note: L.O.I.: loss on ignition

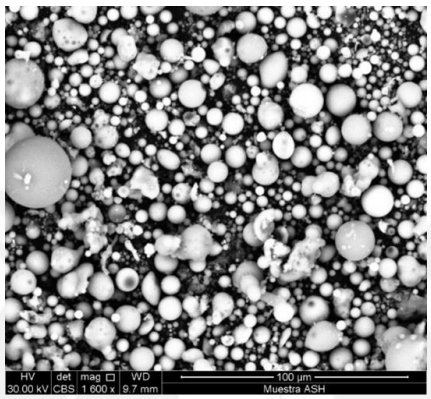

Figure 5.3 Morphology of fly ash particles by scanning electron microscopy (SEM) (FEI-Quanta 650, Thermo Fisher Scientific, USA).

5.2.2 Preparation of geopolymers

The alkaline solution considered a 2.5 weight ratio of Na_2SiO_3 to 8 M NaOH mixed at least one day before the preparation of geopolymers. The 8M NaOH was made as described in Nuruddin, Demie & Ahmed (2011)[1]. *Agave americana* fibers (10 mm) were treated with 1% NaOH concentration over 1 hr. Fiber contents of 0.5%, 0.75% and 1% were added to the geopolymers. Also, a control scenario was considered.

The specimens were prepared using a 0.35 weight ratio of alkaline solution to fly ash. The mixing process was done using a laboratory mixer (UTG-0132, UTEST, Turkey) (Figure 5.4a). The fibers and the fly ash were first mixed (Figure 5.4b), and the alkaline solution was added progressively. The mixing time consisted of ten minutes, five of which were at low speed and the remainder at high speed (Figure 5.4c). After the mixing process (Figure 5.4d), the paste was placed in silicone molds and cured in an oven (Model BD 56, BINDER,

[1]Nuruddin et al. (2011) describe the preparation of an 8M sodium hydroxide solution using 294 g NaOH pellets mixed in 1 kg of solution.

Germany) at 65°C. The blocks were unmolded after 8 hr (Figure 5.4e), and the curing process continued until two days. The mechanical tests were performed at 7 days of age.

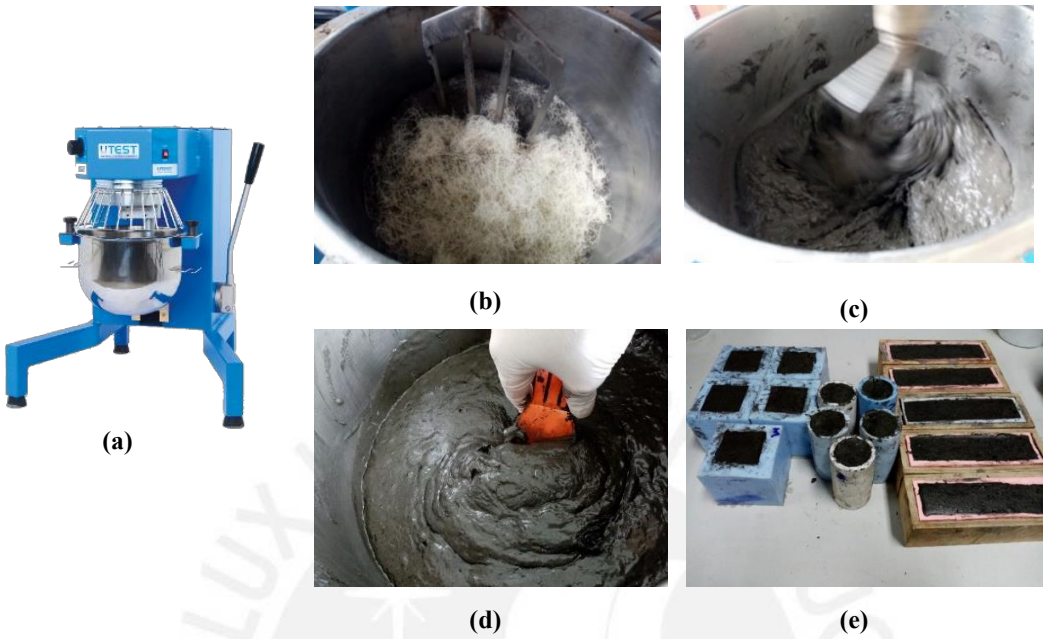

Figure 5.4 Preparation of the fly ash-based geopolymers: (a) laboratory mixer (UTG-0132, UTEST, Turkey), (b) fly ash and agave fibers before the mix, (c) mixing of the geopolymer paste, (d) paste after 10 min of mixing, and (e) geopolymers after 8 hr of curing before unmolding.

5.2.3 Characterization

- **Compressive strength test**

An electromechanical machine (Exceed E45, MTS, USA), with a load capacity of 100 kN (Figure 5.5a), was used for all the mechanical tests. For the compressive strength test, five cubes of 50 mm side (Figure 5.5b) were tested in accordance with the ASTM C109 (ASTM International, 2020b) at 1 mm/min test speed. No capping was considered since the surfaces in contact with the silicone molds were placed at the loading plates. The compressive strength was calculated as follows:

$$fm = \frac{P}{A}$$

where: fm is the compressive strength (MPa), P is the load (N), and A is the area of the loaded surface (mm^2).

The chord modulus of elasticity considering the values of stress and strain of 0.05 and 0.33 the maximum compressive strength (ASTM E111 [ASTM International, 2017]; ASTM

C1314 [ASTM International, 2018]).

- **Flexural strength**

For the flexural strength test, five prisms of 40x40x160 mm (Figure 5.5c) were tested in accordance with the ASTM C348 (ASTM International, 2020a) at 0.1 mm/min test speed. The length between the supports was 120 mm. The blocks whose cracks were found outside the central third of the specimen were discarded. The modulus of rupture or flexural strength was calculated as follows:

$$\boldsymbol{Sf = 0.00028P}$$

where: Sf is the flexural strength (MPa) and P is the total maximum load (N).

- **Splitting tensile strength**

For the splitting tensile strength, five cylinders of 40x80mm (Figure 5.5d) were tested in accordance with the ASTM C496 (ASTM International, 2017) at 0.5 mm/min test speed. Wooden strips of 0.25 mm thick were placed at the surfaces in contact with the loading plates to achieve a suitable load distribution. The splitting tensile strength was calculated as follows:

$$\boldsymbol{T = \frac{2PL}{\pi ld}}$$

Where: T is the indirect tensile strength (MPa), P is the load (N), l is the length (mm), and d is the diameter (mm).

Figure 5.5 Mechanical test for the fly ash-based geopolymers: (a) electromechanical machine (Exceed E45, MTS, USA) (Direct Industry, n.d.-b), (b) specimens for compressive strength, (c) specimens for flexural strength, and (d) specimens for splitting tensile strength test.

- **Morphology of the reinforced geopolymers**

The morphology of the geopolymer was observed using scanning electron microscope SEM (FEI-Quanta 650, Thermo Fisher Scientific, USA) for the reinforced specimens in order to analyze the fiber failure modes. Before the analysis, the specimens were covered with a thin layer of gold and observed at SEM using 10 kV and 75x, 250x, 300x, and 500x magnifications.

5.3 Results and discussion[2]

5.3.1 Compressive strength test

The influence of fibers in the compressive strength of fly ash geopolymers is observed in Figure 5.6a. The compressive strength increased from 14.3 MPa for control blocks to 14.7 MPa, 16.0 MPa, and 15.4 MPa for 0.5%, 0.75%, and 1% fiber content, representing increases of 3%, 12%, and 7%. Notice that the standard deviations show that the 0.75% condition also presents the highest typical ranges. The coefficients of variability are also shown, indicating that the control conditions and 0.5% fiber content are the most heterogeneous.

The results suggest that the compressive strength may increase up to 0.75% fiber content and then start to decrease. Similar trends were found by Alomayri & Low, (2013), who reported increases up to 0.5% fiber content (cotton) in the reinforcement of fly ash-based geopolymers; however, other reported decreases after fiber addition (Chen et al., 2014; Kroehong et al., 2018). The increase in strength was possibly caused by the action of the fibers, which bridged the cracks and led the block to carry more loads (Chen et al., 2014).

Figure 5.6b shows the results of the modulus of elasticity in compression for the fly ash-based geopolymers. The unreinforced blocks obtained a media of 645.4 MPa, and the reinforced specimens increased up to 700.9 MPa, 707.1 MPa, and 732.3 MPa for 0.5%, 0.75% and 1% fiber content. The maximum increase was registered for 1% fiber content, which obtained a value 13% higher than the control specimens.

Figure 5.6c shows the stress-strain curves closest to the average for each condition. The shape of the control condition curve suggests a brittle behavior which is corroborated by the state of the specimens after the test (Figure 5.7 [d], [e], and [f]). The curves of the reinforced blocks, on the other hand, show a ductile behavior, and the specimens remained attached after the test, as shown in Figure 5.7 (g), (h), and (i).

[2] This chapter did not consider boxplots to present the experimental results because its construction requires a sample size greater than five, preferably (Krzywinski & Altman, 2014).

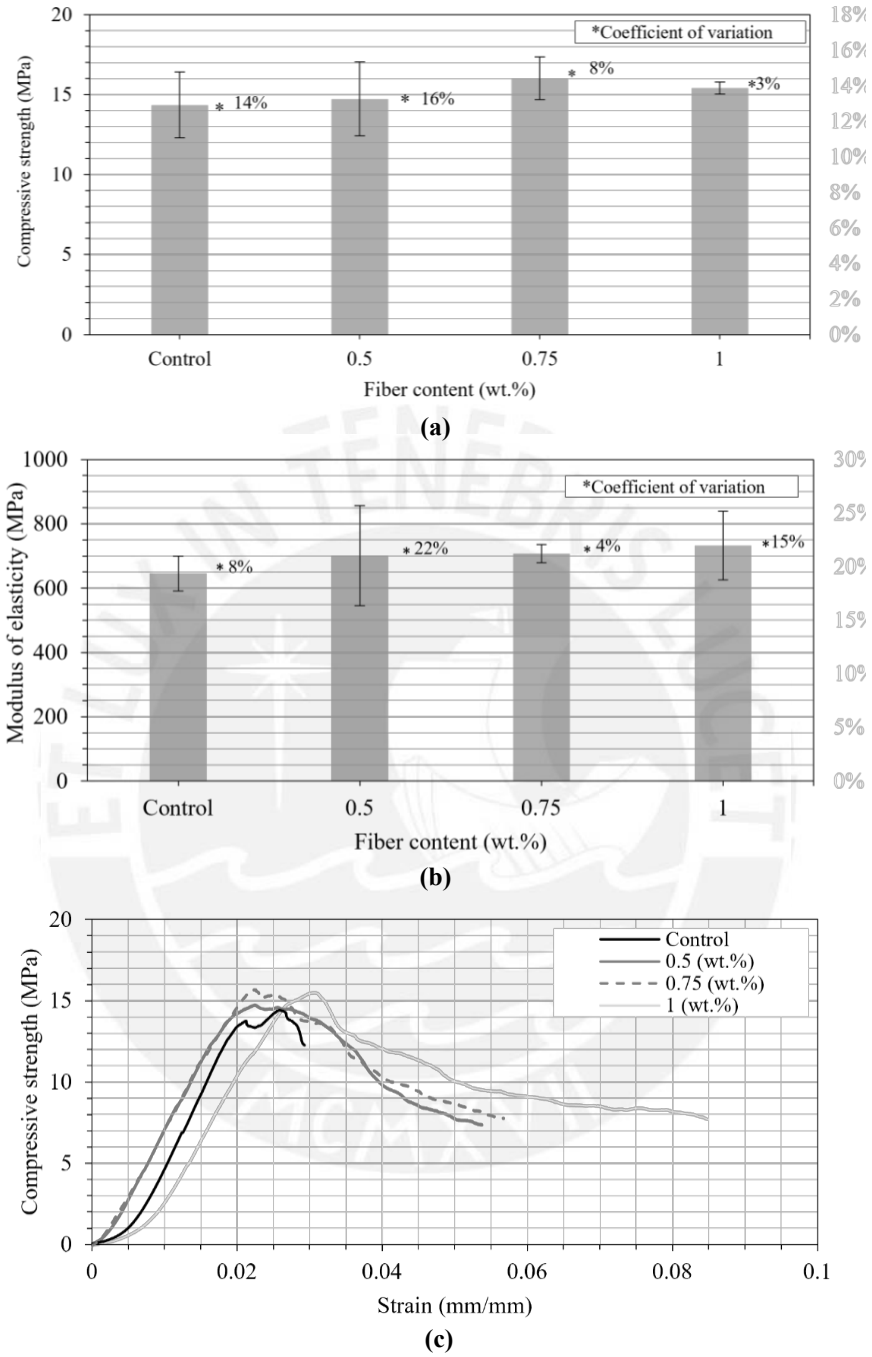

Figure 5.6 Compressive strength test for fly ash-based geopolymers: (a) effect of fiber content on the compressive strength, (b) modulus of elasticity for the compressive test, and (c) strength (MPa)-strain (mm/mm) curves closest to the average.

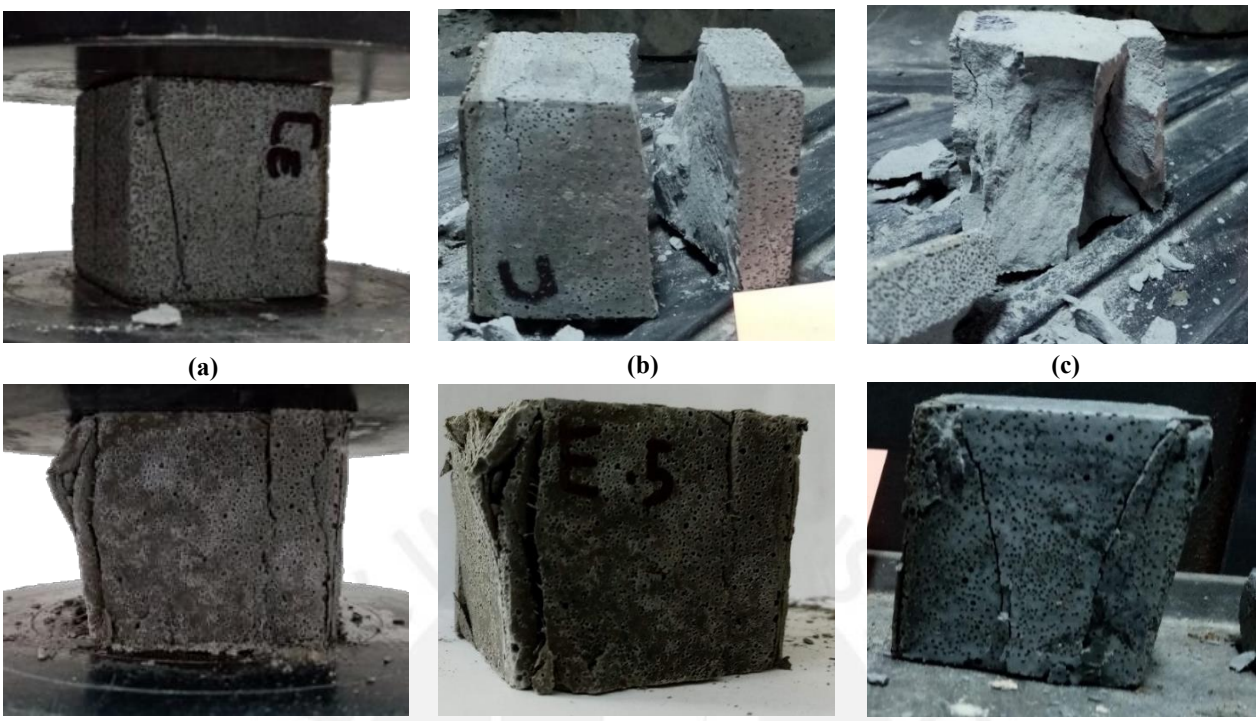

(a) **(b)** **(c)**

(d) **(e)** **(f)**

Figure 5.7 Compressive strength test for the fly ash-based geopolymers: (a), (b), and (c) control specimen after test and (d), (e), and (f) reinforced specimen after the test.

5.3.2 Flexural strength test

The effect of fiber inclusion on flexural strength of fly ash-based geopolymers is seen in Figure 5.8a. The flexural strength decreased from 7.9 MPa for the control case to 6.0 MPa, 6.1 MPa, and 5.6 MPa for 0.5%, 0.75%, and 1% fiber content, representing decreases of 24%, 23%, and 29%. These would suggest that the fibers were not efficient in improving the flexural strength.

The decrease in strength could probably have been caused by the fiber length, which might not be adequate to take the loads and transfer them to the matrix, i.e., they may be working as fillers. Alzeer & MacKenzie (2012) carried experiments with short randomly-oriented wool fibers to reinforce kaolinite-based geopolymers obtaining little or no improvement in the flexural strength. The study also used long fibers (no information about the length), increasing the flexural strength up to 40%. Another factor can be the inclusion of air during the mixing process that produces an inadequate distribution of fibers and stress concentration zones (Alomayri et al., 2013). Korniejenko, Frączek, Pytlak & Adamski (2016) used natural raffia to reinforce fly ash-based geopolymers and reported a decrease

of 45% in the flexural strength as a result of air inclusion.

Figure 5.8b shows the stress-strain curves closest to the average for each condition and Figure 5.9 (c) and (d) show the state of the specimens after testing. Although a brittle behavior is suggested in all conditions, the reinforced specimens remained together after reaching the maximum load, unlike the control blocks that broke into two pieces. A more detailed observation of the crack after the test is observed in Figure 5.9e, in which some fibers can be seen interlacing the fault.

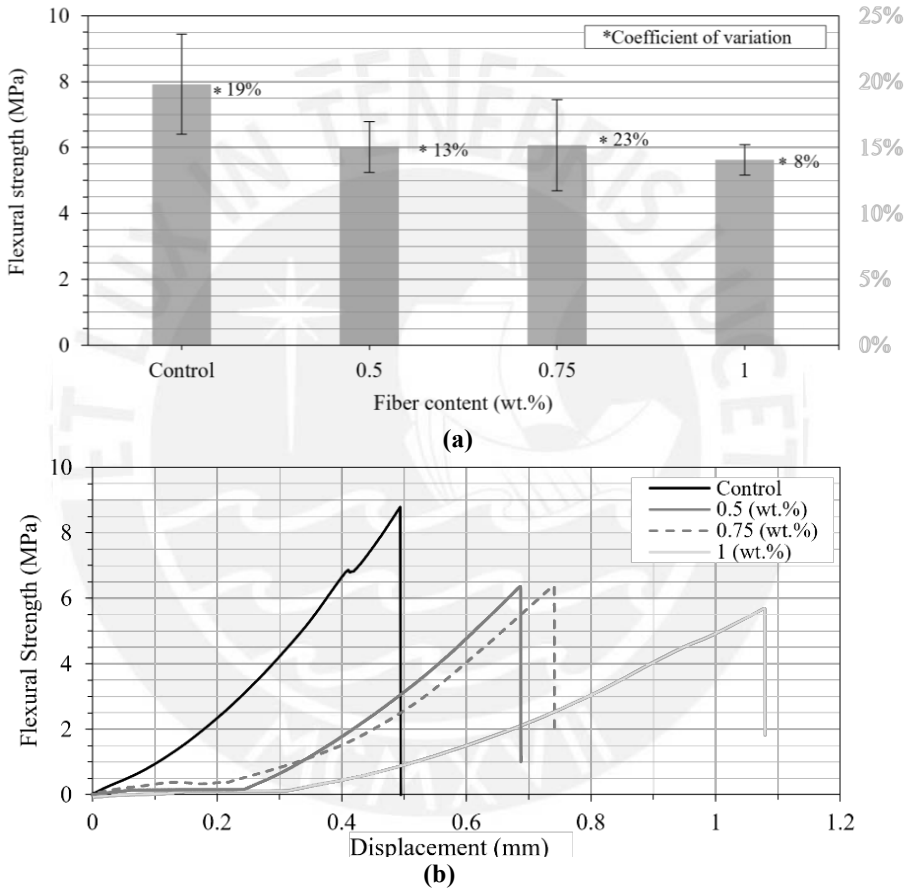

Figure 5.8 Flexural strength test for fly ash-based geopolymers: (a) effect of fiber content on the flexural strength and (b) flexural strength (kN)-displacement (mm) curves closest to the average.

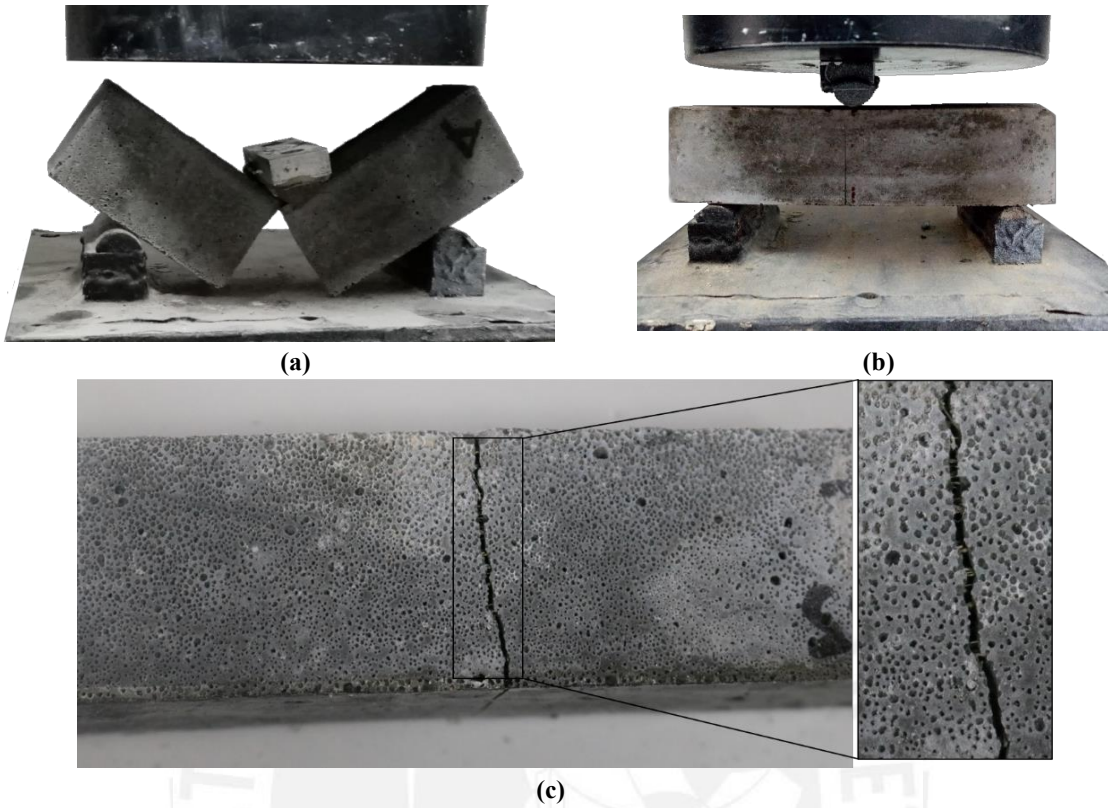

Figure 5.9 Flexural strength test for fly ash-based geopolymers: (a) control specimen after test, (b) reinforced specimen after test and (c) detail of the middle crack for reinforced specimen after the test.

5.3.3 Splitting tensile test

The effect of the inclusion of fibers on the tensile strength of fly ash geopolymers is seen in Figure 5.10a. Tensile strength increased from 1.5 MPa for unreinforced blocks to 1.7 MPa, 1.8 MPa and 2.1 MPa for the 0.5%, 0.75% and 1% fiber content, representing increases of 10%, 16% and 36%. This would suggest that the tensile strength enhances as the addition of fiber increases, which must be caused by the bridging mechanisms fibers develop between the cracks that increase the load capacity of the composite and its ductility. Chen et al. (2014) have also improved the tensile strength of fly ash-based geopolymers by 36% using 2% fiber content (sweet sorghum).

Figure 5.10b shows the tensile strength (MPa)-strain (mm/mm) curves for the control and the optimum fiber content. Reinforced specimens showed a ductile behavior. Figure 5.11 (c) and (d) show the expansion of cracks through the matrix of the reinforced specimen that remained joined after the test, unlike the unreinforced blocks that split into two, as seen in

Figure 5.11 (a) and (b).

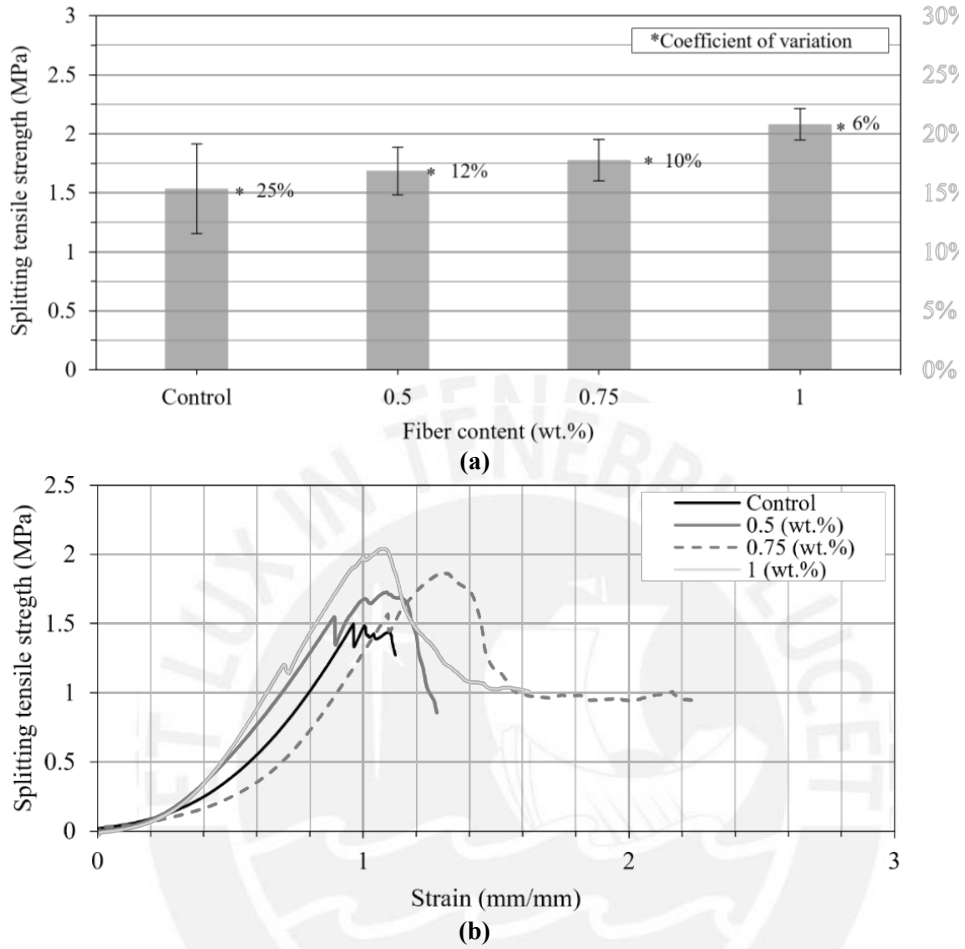

Figure 5.10 Splitting tensile strength test for fly ash geopolymers: (a) effect of fiber content on the splitting tensile strength and (b) strength (MPa)-strain(mm/mm) curves closest to the average.

(a) **(b)**

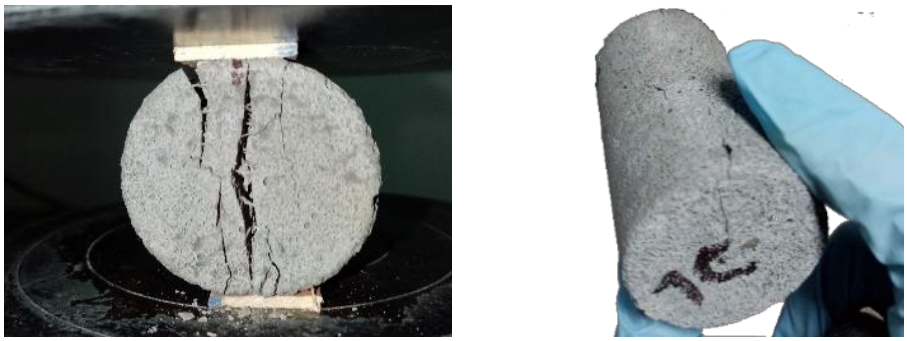

(c) **(d)**

Figure 5.11 Splitting tensile strength test for fly ash geopolymers: (a) control specimen after test and (b) detail of (a), (c) reinforced specimen after test, and (d) detail of (c).

5.3.4 Morphology of the reinforced geopolymers

The mechanical interaction between the agave fiber and the geopolymer matrix is crucial for adequate transfer of loads and good mechanical performance. Figure 5.12 shows the scanning electron microscope (SEM) images for the reinforced geopolymers. The fiber failure modes of pull-out, debonding, and probably fiber breakage can be identified as the main failure modes (see Chapter 3). Figure 5.12a shows signs of the fly-ash geopolymer on the agave fiber surface, indicating a good interfacial adhesion between the elements. This failure mode is known as debonding. It can also be observed some cavities on the matrix indicating the fiber pull-out failure mode. Figure 5.12b shows signs of fiber bending that probably may have caused fiber breakage, another mechanism that helps delay the fracture of the composite.

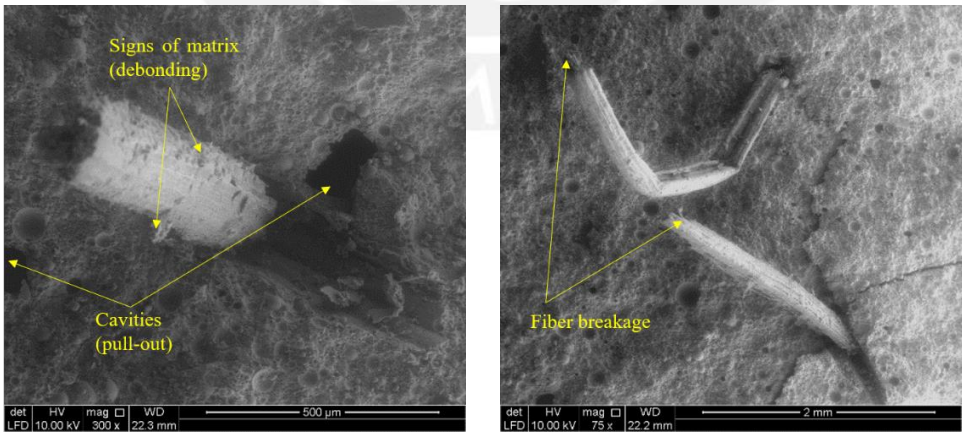

(a) **(b)**

Figure 5.12 Scanning electron microscope (SEM) images of the reinforced fly ash-based geopolymers after the mechanical test: (a) signs of the matrix in the fiber and cavities in the matrix

that suggests debonding and pull-out and (b) fiber breakage.

CHAPTER 6. Conclusions

The results suggest that most agave fibers enhanced their tensile strength and strain after thealkaline treatment. The condition that required minimum resources to improve it efficientlywas 1% NaOH over 1 hr. This condition led to an increase of 87% in respect to the controlstrength of 155 MPa. It also gave the fibers a greater deformation capacity of 217% in respect to 0.12 mm obtained for control fibers. For this condition, the modulus of elasticity decreased by about 50% after treatment. On the other hand, SEM images allowed to verify the changes on the fiber surface, identifying 20 % NaOH over 3 hr as an aggressive condition that could weaken the agave fiber.

The agave fibers treated at the suggested condition were used to reinforce fly ash-based geopolymers. During the tests, it was observed that fibers enhanced crack propagation, which may be a responsible mechanism for an increased load capacity in some mechanical tests, e.g., compressive and splitting tensile strength. In contrast, control geopolymers showed brittle behavior breaking into pieces after the tests. By SEM, fiber debonding, pull-out and signs of fiber breakage were identified as some of the bridging mechanisms that lead to shifting the failure mode from brittle to ductile.

After reinforcement, the compressive strength increased up to 0.75% fiber content (+12%), and the modulus of elasticity registered a constant increase until the maximum fiber content of 1% (+13%). However, contrary to expectations, the flexural strength was not enhanced, being the maximum decrease of 29% for 1% fiber content. Therefore, further work is required to understand the influence of other factors such as fiber length. On the other hand, the splitting tensile strength was enhanced up to 1% fiber content (+36%).

As it is known, flexural and splitting tensile strength tests lead to estimate the tensile strength of the composite indirectly; however, for the study, the obtained trends were different. Empirical relationships have not yet been developed for natural fiber reinforced cementitious composites; still, there are some for synthetic fibers, such as the case of steel (Xu & Shi, 2009) and, certainly, for conventional concrete (American Concrete Pavement Associations, n.d.), the last which were used correlate not only flexural and splitting tensile strength results but also those of compressive in the present study. The obtained results mostly comply with compressive and splitting tensile correlations; however, this was not the case for flexural strength. Thus, it is suggested to extend the experimental campaign, including other parameters such as

the fiber length, as mentioned before, and other natural fibers and cementitious matrices. The studies should also aim to obtain empirical correlations between the mechanical properties of the natural fiber reinforced composite.

Additional recommendations:

- The standard grips used in the mechanical characterization produced the consecutive slippage of fibers. In the early stage of the experimentation, some efforts were made to overcome this issue. First, a moldable putty Moldimix (SOLDIMIX, Peru) was used to glue the fibers to the mounting tabs and thus produce a kind of anchor at the extremes of the specimen. Later, super glue was used and had the same effects. The procedures, however, required time. Other grip models are commercially available, which are, in effect, designed for the testing of fibers.
- It is also recommended to study the water absorption change after the alkaline treatment since it can also influence the reinforcement of cementitious matrices. Chemical tests should also be performed to identify the content of components after treatment and X-ray diffraction techniques to identify the degree of crystallinity and microfibrillar angles. A durability study is also needed to understand the effects of the alkaline medium in the long term.
- Fiber contents higher than 1% could cause workability issues and require the use of water. In the early experimentation stage, trials consider a condition of 1.25% fiber content, but the mixture had poor workability.
- About the curing process of geopolymers, the unmolding time after 2 hr of thermal curing was considered in the early stage, but it was observed that after completing two days, the blocks had poor quality and were easily crumbled when manipulated. Unmolding under the described conditions is not recommended.

References

Ahmari, S., & Zhang, L. (2012). Production of eco-friendly bricks from copper mine tailings through geopolymerization. Construction and Building Materials, 29, 323–331. https://doi.org/10.1016/j.conbuildmat.2011.10.048

Ajouguim, S., Abdelouahdi, K., Waqif, M., Stefanidou, M., & Saâdi, L. (2019). Modifications of Alfa fibers by alkali and hydrothermal treatment. Cellulose, 26(3), 1503–1516. https://doi.org/10.1007/s10570-018-2181-9

Alomayri, T., Assaedi, H., Shaikh, F. U. A., & Low, I. M. (2014). Effect of water absorption on the mechanical properties of cotton fabric-reinforced geopolymer composites. Journal of Asian Ceramic Societies, 2(3), 223–230. https://doi.org/10.1016/j.jascer.2014.05.005

Alomayri, T., & Low, I. M. (2013). Synthesis and characterization of mechanical properties in cotton fiber-reinforced geopolymer composites. Journal of Asian Ceramic Societies, 1(1), 30–34. https://doi.org/10.1016/j.jascer.2013.01.002

Alves Fidelis, M. E., Pereira, T. V. C., Gomes, O. da F. M., de Andrade Silva, F., & Toledo Filho, R. D. (2013). The effect of fiber morphology on the tensile strength of natural fibers. Journal of Materials Research and Technology, 2(2), 149–157. https://doi.org/10.1016/j.jmrt.2013.02.003

Alzeer, M., & MacKenzie, K. (2013). Synthesis and mechanical properties of novel composites of inorganic polymers (geopolymers) with unidirectional natural flax fibres (phormium tenax). Applied Clay Science, 75–76, 148–152. https://doi.org/10.1016/j.clay.2013.03.010

Alzeer, M., & MacKenzie, K. J. D. (2012). Synthesis and mechanical properties of new fibre-reinforced composites of inorganic polymers with natural wool fibres. Journal of Materials Science, 47(19), 6958–6965. https://doi.org/10.1007/s10853-012-6644-3

Amel, B. A., Paridah, M. T., Sudin, R., Anwar, U. M. K., & Hussein, A. S. (2013). Effect of fiber extraction methods on some properties of kenaf bast fiber. Industrial Crops and Products, 46, 117–123. https://doi.org/10.1016/j.indcrop.2012.12.015

American Concrete Institute (ACI). (2002a). Report on Fiber Reinforced Concrete.

References

Reported by ACI Committee 544 (Vol. 96, Issue Reapproved).

American Concrete Institute (ACI). (2002b). Report on Fiber Reinforced Concrete.

American Concrete Pavement Associations. (n.d.). What are the strength tests? Retrieved May 25, 2021, from http://1204075.sites.myregisteredsite.com/Concrete_Pavement/Technical/FATQ/Construction/Strength_Tests.asp

Andrew, R. M. (2019). Global CO 2 emissions from cement production, 1928-2018. Earth Syst. Sci. Data, 11, 1675–1710. https://doi.org/10.5194/essd-11-1675-2019

ASTM International. (2014). Standard Test Method for Tensile Strength and Young's Modulus of Fibers. In Astm C1557-14. https://doi.org/10.1520/C1557-14.2

ASTM E111 - 17 Standard Test Method for Young's Modulus, Tangent Modulus, and Chord Modulus, (2017). https://doi.org/10.1520/E0111-17

ASTM International. (2017). Standard Test Method for Splitting Tensile Strength of Cylindrical Concrete Specimens. https://doi.org/10.1520/C0496_C0496M-17

ASTM C1314 - 18 Standard Test Method for Compressive Strength of Masonry Prisms, (2018). https://doi.org/10.1520/C1314-18

ASTM International. (2019). ASTM C618-19 Standard Specification for Coal Fly Ash and Raw or Calcined Natural Pozzolan for Use in Concrete. https://doi.org/10.1520/C0618-19

ASTM International. (2020a). ASTM C348 - 20 Standard Test Method for Flexural Strength of Hydraulic-Cement Mortars. https://doi.org/10.1520/C0348-20

ASTM International. (2020b). Standard Test Method for Compressive Strength of Hydraulic Cement Mortars (Using 2-in. or [50 mm] Cube Specimens). https://doi.org/10.1520/C0109_C0109M-20B

Bessadok, A., Marais, S., Roudesli, S., Lixon, C., & Métayer, M. (2008). Influence of chemical modifications on water-sorption and mechanical properties of Agave fibres. Composites Part A: Applied Science and Manufacturing, 39(1), 29–45. https://doi.org/10.1016/j.compositesa.2007.09.007

Bezazi, A., Belaadi, A., Bourchak, M., Scarpa, F., & Boba, K. (2014). Novel extraction

References

techniques, chemical and mechanical characterisation of Agave americana L. natural fibres. Composites Part B: Engineering, 66, 194–203. https://doi.org/10.1016/j.compositesb.2014.05.014

Cai, M., Takagi, H., Nakagaito, A. N., Li, Y., & Waterhouse, G. I. N. (2016). Effect of alkali treatment on interfacial bonding in abaca fiber-reinforced composites. Composites Part A: Applied Science and Manufacturing, 90, 589–597. https://doi.org/10.1016/j.compositesa.2016.08.025

Camargo, M. M., Taye, E. A., Roether, J. A., Redda, D. T., & Boccaccini, A. R. (2020). A review on natural fiber-reinforced geopolymer and cement-based composites. In Materials (Vol. 13, Issue 20, pp. 1–29). MDPI AG. https://doi.org/10.3390/ma13204603

Célino, A., Fréour, S., Jacquemin, F., & Casari, P. (2014a). The hygroscopic behavior of plant fibers: A review. Frontiers in Chemistry, 1(JAN), 43. https://doi.org/10.3389/fchem.2013.00043

Célino, A., Fréour, S., Jacquemin, F., & Casari, P. (2014b). The hygroscopic behavior of plant fibers: A review. Frontiers in Chemistry, 1(JAN), 43. https://doi.org/10.3389/fchem.2013.00043

Chaabouni, Y., Drean, J. Y., Msahli, S., & Sakli, F. (2006). Morphological Characterization of Individual Fiber of Agave americana L. Textile Research Journal, 76(5), 367–374. https://doi.org/10.1177/0040517506061965

Chen, H., Yu, Y., Zhong, T., Wu, Y., Li, Y., Wu, Z., & Fei, B. (2017). Effect of alkali treatment on microstructure and mechanical properties of individual bamboo fibers. Cellulose, 24(1), 333–347. https://doi.org/10.1007/s10570-016-1116-6

Chen, R., Ahmari, S., & Zhang, L. (2014). Utilization of sweet sorghum fiber to reinforce fly ash-based geopolymer. Journal of Materials Science, 49(6), 2548–2558. https://doi.org/10.1007/s10853-013-7950-0

Cheng, T. W., & Chiu, J. P. (2003). Fire-resistant geopolymer produce by granulated blast furnace slag. Minerals Engineering, 16(3), 205–210. https://doi.org/10.1016/S0892-6875(03)00008-6

Concrete Technology Weblog. (2008). Principles Governing FRC.

References

https://caementitium.wordpress.com/2008/01/31/principles-governing-frc/

Davidovits, J. (2017). Geopolymers: Ceramic-like inorganic polymers. In Journal of Ceramic Science and Technology (Vol. 8, Issue 3, pp. 335–350). Goller Verlag. https://doi.org/10.4416/JCST2017-00038

Davidovits, Joseph; (2018). Why Alkali-Activated Materials (AAM) are not Geopolymers ? Vol. Technical. https://doi.org/10.13140/RG.2.2.34337.25441

Davidovits, Joseph. (1994). GEOPOLYMERS: Man-Made Rock Geosynthesis and the Resulting Development of Very Early High Strength Cement. Journal of Materials Education, 16(3), 91–139.

Davidovits, Joseph. (2008). They Built the Pyramids. In They Built the Pyramids. Geopolymer Institute. https://books.google.es/books?hl=es&lr=&id=voDCTESa04kC&oi=fnd&pg=PA1&dq=joseph+davidovits+they+built+the+piramids&ots=7_hSsimI93&sig=bKSkO5FBQaVlrqSYGAaqAnBwGIY#v=onepage&q=joseph davidovits they built the piramids&f=false

Davidovits, Joseph. (2015). Geopolymer Chemistry and Applications. In Joseph Davidovits (Ed.), Geopolymer Chemistry and Applications (5th ed.). Geopolymer Institute.

Davidovits, Joseph, Huaman, L., & Davidovits, R. (2019). Ancient geopolymer in south-American monument. SEM and petrographic evidence. Materials Letters, 235, 120–124. https://doi.org/10.1016/j.matlet.2018.10.033

Direct Industry. (n.d.-a). Máquina de prueba multi-parámetros - max. 5kN Exceed E42 - MTS Systems (China) CO., Ltd. - de materiales / electromecánica / estática. N.D. Retrieved April 4, 2021, from https://www.directindustry.es/prod/mts-systems-china-co-ltd/product-54100-1164881.html

Direct Industry. (n.d.-b). Máquina de prueba universal - max. 300 kN | Exceed E45 - MTS Systems (China) CO., Ltd. - multi-parámetros / para materiales. Retrieved April 4, 2021, from https://www.directindustry.es/prod/mts-systems-china-co-ltd/product-54100-1158083.html

Djafari Petroudy, S. R. (2017). Physical and mechanical properties of natural fibers. In

References

Advanced High Strength Natural Fibre Composites in Construction (pp. 59–83). Elsevier Inc. https://doi.org/10.1016/B978-0-08-100411-1.00003-0

El Oudiani, A., Ben Sghaier, R., Chaabouni, Y., Msahli, S., & Sakli, F. (2012). Physico-chemical and mechanical characterization of alkali-treated Agave americana L. fiber. Journal of the Textile Institute, 103(4), 349–355. https://doi.org/10.1080/00405000.2011.578358

Fernández-Jiménez, A., & Palomo, A. (2003). Characterisation of fly ashes. Potential reactivity as alkaline cements. In Fuel (Vol. 82, Issue 18). https://doi.org/10.1016/S0016-2361(03)00194-7

Fernández, A., Palomo, A., & Criado, M. (2006). Activación alcalina de cenizas volantes. Estudio comparativo entre activadores sódicos y potásicos. 56(281), 51–65. https://doi.org/10.3989/mc.2008.v58.i291.101

Geopolymer Institute. (2014). Alkali activated materials are not geopolymer-Part 1. https://www.youtube.com/watch?v=3QGUCHt0tDs&t=253s

Gholampour, A., & Ozbakkaloglu, T. (2019). A review of natural fiber composites: properties, modification and processing techniques, characterization, applications. In Journal of Materials Science (Vol. 55, Issue 3, pp. 829–892). Springer New York LLC. https://doi.org/10.1007/s10853-019-03990-y

Global Invasive Species Database. (2020). Agave Americana. In Journal of Chemical Information and Modeling (Vol. 21, Issue 1). http://www.iucngisd.org/gisd/species.php?sc=1664

Gomez, L. (2015). Obtencion experimental de nuevas fibras vegetales. dspace.uazuay.edu.ec

Görhan, G., & Kürklü, G. (2014). The influence of the NaOH solution on the properties of the fly ash-based geopolymer mortar cured at different temperatures. Composites Part B: Engineering, 58, 371–377. https://doi.org/10.1016/j.compositesb.2013.10.082

Hardjito, D., & Rangan, B. V. (2005). DEVELOPMENT AND PROPERTIES OF LOW-CALCIUM FLY ASH-BASED GEOPOLYMER CONCRETE.

He, J., Jie, Y., Zhang, J., Yu, Y., & Zhang, G. (2013). Synthesis and characterization

References

of red mud and rice husk ash-based geopolymer composites. Cement and Concrete Composites, 37(1), 108–118. https://doi.org/10.1016/j.cemconcomp.2012.11.010

Hulle, A., Kadole, P., & Katkar, P. (2015). Agave Americana leaf fibers. Fibers, 3(1), 64–75. https://doi.org/10.3390/fib3010064

Imbabi. (2013). Trends and developments in green cement and concrete technology. https://www.sciencedirect.com/science/article/pii/S2212609013000071

Indran, S., & Raj, R. E. (2015). Characterization of new natural cellulosic fiber from Cissus quadrangularis stem. Carbohydrate Polymers, 117, 392–399. https://doi.org/10.1016/j.carbpol.2014.09.072

International Energy Agency. (2019). Coal 2019 – Analysis - IEA. https://www.iea.org/reports/coal-2019

Juarez, C. (2002). Concretos base cemento portland reforzados con fibras naturales(agave lecheguilla), como materiales para construcción en México.

Kestur G., S., Flores-Sahagun, T. H. S., Dos Santos, L. P., Dos Santos, J., Mazzaro, I., & Mikowski, A. (2013). Characterization of blue agave bagasse fibers of Mexico. Composites Part A: Applied Science and Manufacturing, 45, 153–161. https://doi.org/10.1016/j.compositesa.2012.09.001

Komljenović, M., Baščarević, Z., & Bradić, V. (2010). Mechanical and microstructural properties of alkali-activated fly ash geopolymers. Journal of Hazardous Materials, 181(1–3), 35–42. https://doi.org/10.1016/j.jhazmat.2010.04.064

Korniejenko, K., Frączek, E., Pytlak, E., & Adamski, M. (2016). Mechanical Properties of Geopolymer Composites Reinforced with Natural Fibers. Procedia Engineering, 151, 388–393. https://doi.org/10.1016/j.proeng.2016.07.395

Kroehong, W., Jaturapitakkul, C., Pothisiri, T., & Chindaprasirt, P. (2018). Effect of Oil Palm Fiber Content on the Physical and Mechanical Properties and Microstructure of High-Calcium Fly Ash Geopolymer Paste. Arabian Journal for Science and Engineering, 43(10), 5215–5224. https://doi.org/10.1007/s13369-017-3059-0

References

Krzywinski, M., & Altman, N. (2014). Visualizing samples with box plots. Nature Methods, 11(2), 119–120. https://doi.org/10.1038/nmeth.2813

Kupwade-Patil, K., & Allouche, E. N. (2013). Impact of Alkali Silica Reaction on Fly Ash-Based Geopolymer Concrete. Journal of Materials in Civil Engineering, 25(1), 131–139. https://doi.org/10.1061/(ASCE)MT.1943-5533.0000579

Lazorenko, G., Kasprzhitskii, A., Yavna, V., Mischinenko, V., Kukharskii, A., Kruglikov, A., Kolodina, A., & Yalovega, G. (2020). Effect of pre-treatment of flax tows on mechanical properties and microstructure of natural fiber reinforced geopolymer composites. Environmental Technology and Innovation, 20, 101105. https://doi.org/10.1016/j.eti.2020.101105

Lee, C. H., Khalina, A., Lee, S. H., & Liu, M. (2020). A Comprehensive Review on Bast Fibre Retting Process for Optimal Performance in Fibre-Reinforced Polymer Composites. In Advances in Materials Science and Engineering (Vol. 2020). Hindawi Limited. https://doi.org/10.1155/2020/6074063

Liu, W., Mohanty, A. K., Drzal, L. T., Askel, P., & Misra, M. (2004). Effects of alkali treatment on the structure, morphology and thermal properties of native grass fibers as reinforcements for polymer matrix composites. Journal of Materials Science, 39(3), 1051–1054. https://doi.org/10.1023/B:JMSC.0000012942.83614.75

Löfgren, I. (2005). Fibre-reinforced Concrete for Industrial Construction [Chalmers University of Technology]. https://core.ac.uk/download/pdf/70560762.pdf

Machaka, M., Abou Chakra, H., & Elkordi Professor, A. (2014). Alkali Treatment of Fan Palm Natural Fibers for Use in Fiber Reinforced Concrete. European Scientific Journal, 10(12), 1857–7881.

Malenab, R., Ngo, J., & Promentilla, M. (2017). Chemical Treatment of Waste Abaca for Natural Fiber-Reinforced Geopolymer Composite. Materials, 10(6), 579. https://doi.org/10.3390/ma10060579

Martínez-López, C., Mejía-Arcila, J. M., Torres-Agredo, J., & Mejía-De Gutiérrez, R. (2015). Evaluation of the toxicity characteristics of two industrial wastes valorized by geopolymerization process. DYNA, 82, 74–81.

References

https://doi.org/10.15446/dyna.v82n190.43136

Mejía, J. M., Rodríguez, E. D., & De Gutiérrez, R. M. (2014). Utilización potencial de una ceniza volante de baja calidad como fuente de aluminosilicatos en la producción de geopolímeros. Ingenieria y Universidad, 18(2), 309–327. https://doi.org/10.11144/Javeriana.IYU18-2.upcv

Merta, I., & Tschegg, E. K. (2013). Fracture energy of natural fibre reinforced concrete. Construction and Building Materials, 40, 991–997. https://doi.org/10.1016/j.conbuildmat.2012.11.060

Mori, S., Tenazoa, C., Candiotti, S., Flores, E., & Charca, S. (2018). Assessment of Ichu Fibers Extraction and Their Use as Reinforcement in Composite Materials. Journal of Natural Fibers, 00(00), 1–16. https://doi.org/10.1080/15440478.2018.1527271

Noushini, A., Hastings, M., Castel, A., & Aslani, F. (2018). Mechanical and flexural performance of synthetic fibre reinforced geopolymer concrete. Construction and Building Materials, 186, 454–475. https://doi.org/10.1016/j.conbuildmat.2018.07.110

Palomo, A., & Palacios, M. (2003). Alkali-activated cementitious materials: Alternative matrices for the immobilisation of hazardous wastes - Part II. Stabilisation of chromium and lead. In Cement and Concrete Research (Vol. 33, Issue 2). Pergamon. https://doi.org/10.1016/S0008-8846(02)00964-X

Pickering, K. L., Efendy, M. G. A., & Le, T. M. (2016). A review of recent developments in natural fibre composites and their mechanical performance. Composites Part A: Applied Science and Manufacturing, 83, 98–112. https://doi.org/10.1016/j.compositesa.2015.08.038

Ramamoorthy, S. K., Skrifvars, M., & Persson, A. (2015). A review of natural fibers used in biocomposites: Plant, animal and regenerated cellulose fibers. In Polymer Reviews (Vol. 55, Issue 1, pp. 107–162). Taylor and Francis Inc. https://doi.org/10.1080/15583724.2014.971124

Rangan, V. (2014). Geopolymer concrete for environmental protection. https://www.geopolymer.org/fichiers_pdf/FA-GP-Concrete.pdf

References

Rattanasak, U., & Chindaprasirt, P. (2009). Influence of NaOH solution on the synthesis of fly ash geopolymer. Minerals Engineering, 22(12), 1073–1078. https://doi.org/10.1016/j.mineng.2009.03.022

Ray, D., & Sarkar, B. K. (2001). Characterization of alkali-treated jute fibers for physical and mechanical properties. Journal of Applied Polymer Science, 80(7), 1013–1020. https://doi.org/10.1002/app.1184

Rocha, S., Andrade, F. De, Roberto, P., Lima, L., Dias, R., & Filho, T. (2015). Effect of fiber treatments on the sisal fiber properties and fiber – matrix bond in cement based systems. CONSTRUCTION & BUILDING MATERIALS, 101, 730–740. https://doi.org/10.1016/j.conbuildmat.2015.10.120

Roel, P., Hernández, M. A., & Huamaní, I. (n.d.). El Q'eswachaka de Canas. Ingeniería y tradición en las comunidades de Quehue.

Sá Ribeiro, R. A., Sá Ribeiro, M. G., Sankar, K., & Kriven, W. M. (2016). Geopolymer-bamboo composite – A novel sustainable construction material. Construction and Building Materials, 123, 501–507. https://doi.org/10.1016/j.conbuildmat.2016.07.037

Sagawa, Y., Ota, S., Harada, K., Nishizaki, T., & Goda, H. (2015). Utilization of Fly Ash with Higher Loss on Ignition for Geopolymer Mortar. Advanced Materials Research, 1129, 614–620. https://doi.org/10.4028/www.scientific.net/amr.1129.614

Saha, P., Manna, S., Chowdhury, S. R., Sen, R., Roy, D., & Adhikari, B. (2010). Enhancement of tensile strength of lignocellulosic jute fibers by alkali-steam treatment. Bioresource Technology, 101(9), 3182–3187. https://doi.org/10.1016/J.BIORTECH.2009.12.010

Salih, M. M., Osofero, A. I., & Imbabi, M. S. (2020). Critical review of recent development in fiber reinforced adobe bricks for sustainable construction. https://doi.org/10.1007/s11709-020-0630-7

Sarker, P. K., Kelly, S., & Yao, Z. (2014). Effect of fire exposure on cracking, spalling and residual strength of fly ash geopolymer concrete. Materials and Design, 63, 584–592. https://doi.org/10.1016/j.matdes.2014.06.059

References

Sedan, D., Pagnoux, C., Smith, A., & Chotard, T. (2008). Mechanical properties of hemp fibre reinforced cement: Influence of the fibre/matrix interaction. Journal of the European Ceramic Society, 28, 183–192. https://doi.org/10.1016/j.jeurceramsoc.2007.05.019

Silva, G. (2018). Development of an eco-friendly composite based on geopolymer matrix produced with fired clay brick powder and reinforced with natural fibers (thesis of master degree). http://tesis.pucp.edu.pe/repositorio/handle/20.500.12404/766/browse?type=author&value=Silva+Mondragón%2C+Guido+Leonardo

Silva, G., Kim, S., Bertolotti, B., Nakamatsu, J., & Aguilar, R. (2020). Optimization of a reinforced geopolymer composite using natural fibers and construction wastes. Construction and Building Materials, 258, 119697. https://doi.org/10.1016/j.conbuildmat.2020.119697

Silva Santos, L., Hernández-Gómez, L. H., Caballero-Caballero, M., & López-Hernández, I. (2009). Tensile strength of fibers extracted from the leaves of the angustifolia Haw agave in function of their length. Applied Mechanics and Materials, 15, 103–108. https://doi.org/10.4028/www.scientific.net/AMM.15.103

Sindhunata, Van Deventer, J. S. J., Lukey, G. C., & Xu, H. (2006). Effect of curing temperature and silicate concentration on fly-ash-based geopolymerization. Industrial and Engineering Chemistry Research, 45(10), 3559–3568. https://doi.org/10.1021/ie051251p

Sisti, L., Totaro, G., Vannini, M., & Celli, A. (2018). Retting Process as a Pretreatment of Natural Fibers for the Development of Polymer Composites (pp. 97–135). Springer, Cham. https://doi.org/10.1007/978-3-319-68696-7_2

Sukmak, P., De Silva, P., Horpibulsuk, S., & Chindaprasirt, P. (2015). Sulfate Resistance of Clay-Portland Cement and Clay High-Calcium Fly Ash Geopolymer. Journal of Materials in Civil Engineering, 27(5), 04014158. https://doi.org/10.1061/(ASCE)MT.1943-5533.0001112

Thirumalaisamy, R., & Pavayee Subramani, S. (2018). Investigation of physico-

References

mechanical and moisture absorption characteristics of raw and alkali treated new agave angustifolia marginata (AAM) fiber. Medziagotyra, 24(1), 53–58. https://doi.org/10.5755/j01.ms.24.1.17542

US Department of Transportation Federal Highway Administration. (2004). TechBrief: Geopolymer Concrete.

Van Jaarsveld, J. G. S., & Van Deventer, J. S. J. (1999). Effect of metal contaminants on the formation and properties of waste-based geopolymers. Cement and Concrete Research, 29(8), 1189–1200. https://doi.org/10.1016/S0008-8846(99)00032-0

Vasquez, J. Z., Romel, C., Patalud, S., Tarnate, P. M. O., Ramirez, S. G., Escobar, E. C., & Vaso, C. C. (2016). Effect of alkali treatment on the mechanical, physical, and thermal properties of sweet sorghum [Sorghum bicolor (L.) Moench] fibers. Philippine E-Journal for Applied Research and Development, 6, 1–9. http://pejard.slu.edu.ph/vol.6/2016.03.08.pdf

Vera, J. (2009). Filamentos de carbono en hormigones. Boletín Del Grupo Español Del Carbón, 1–7. https://dialnet.unirioja.es/descarga/articulo/3986764.pdf

Wattimena, O. K., & Hardjito, D. (2017). A review on the effect of fly ash characteristics and their variations on the synthesis of fly ash based geopolymer ARTICLES YOU MAY BE INTERESTED IN A Review on the Effect of Fly Ash Characteristics and Their Variations on the Synthesis of Fly Ash Based Geopolymer. 1887, 20041. https://doi.org/10.1063/1.5003524

Williamson, D F, Parker, R A, & Kendrick, J S. (1989). The box plot: a simple visual method to interpret data. Annals of Internal Medicine, 110(11), 916–921.

Xu, B. W., & Shi, H. S. (2009). Correlations among mechanical properties of steel fiber reinforced concrete. Construction and Building Materials, 23(12), 3468–3474. https://doi.org/10.1016/j.conbuildmat.2009.08.017

Yan, L., Chouw, N., Huang, L., & Kasal, B. (2016). Effect of alkali treatment on microstructure and mechanical properties of coir fibres, coir fibre reinforced-polymer composites and reinforced-cementitious composites. Construction and Building Materials, 112, 168–182.

References

https://doi.org/10.1016/j.conbuildmat.2016.02.182

Yan, L., Kasal, B., & Huang, L. (2016). A review of recent research on the use of cellulosic fibres, their fibre fabric reinforced cementitious, geo-polymer and polymer composites in civil engineering. Composites Part B: Engineering, 92, 94–132. https://doi.org/10.1016/J.COMPOSITESB.2016.02.002

Zhuang, H. J., Zhang, H. Y., & Xu, H. (2017). Resistance of geopolymer mortar to acid and chloride attacks. Procedia Engineering, 210, 126–131. https://doi.org/10.1016/j.proeng.2017.11.057

Zhuang, X. Y., Chen, L., Komarneni, S., Zhou, C. H., Tong, D. S., Yang, H. M., Yu, W. H., & Wang, H. (2016). Fly ash-based geopolymer: Clean production, properties and applications. In Journal of Cleaner Production (Vol. 125, pp. 253–267). Elsevier Ltd. https://doi.org/10.1016/j.jclepro.2016.03.019

Zollo, R. F. (1997). Fiber-reinforced concrete: An overview after 30 years of development. In Cement and Concrete Composites (Vol. 19, Issue 2, pp. 107–122). Elsevier. https://doi.org/10.1016/s0958-9465(96)00046-7

APPENDIX I: Chapter 4 – Photos of the experimental stage

I.A. Measurement of fiber diameter by optical microscope (DM750, Leica, Germany)

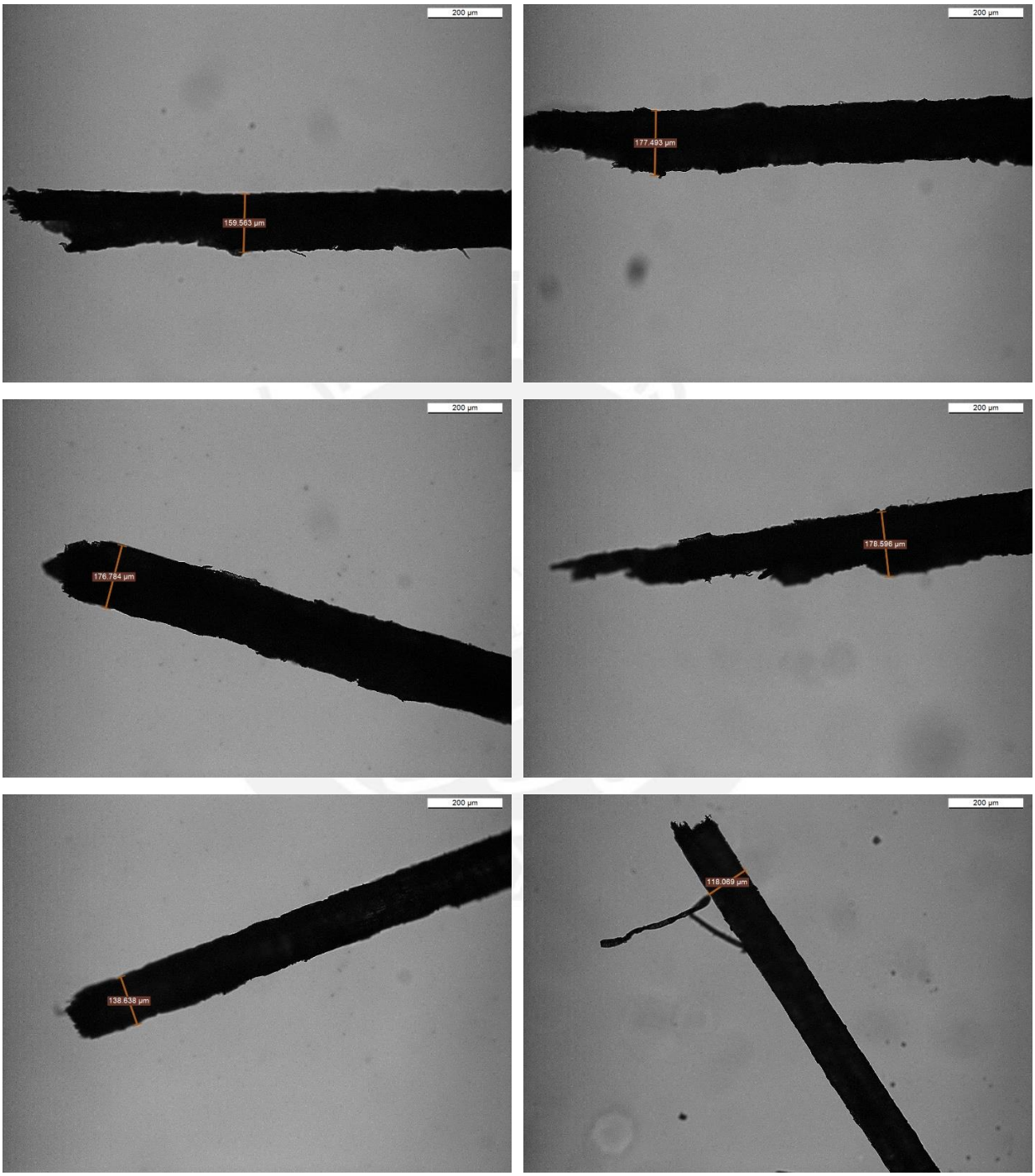

Measurement of the fiber diameter after the tensile strength test

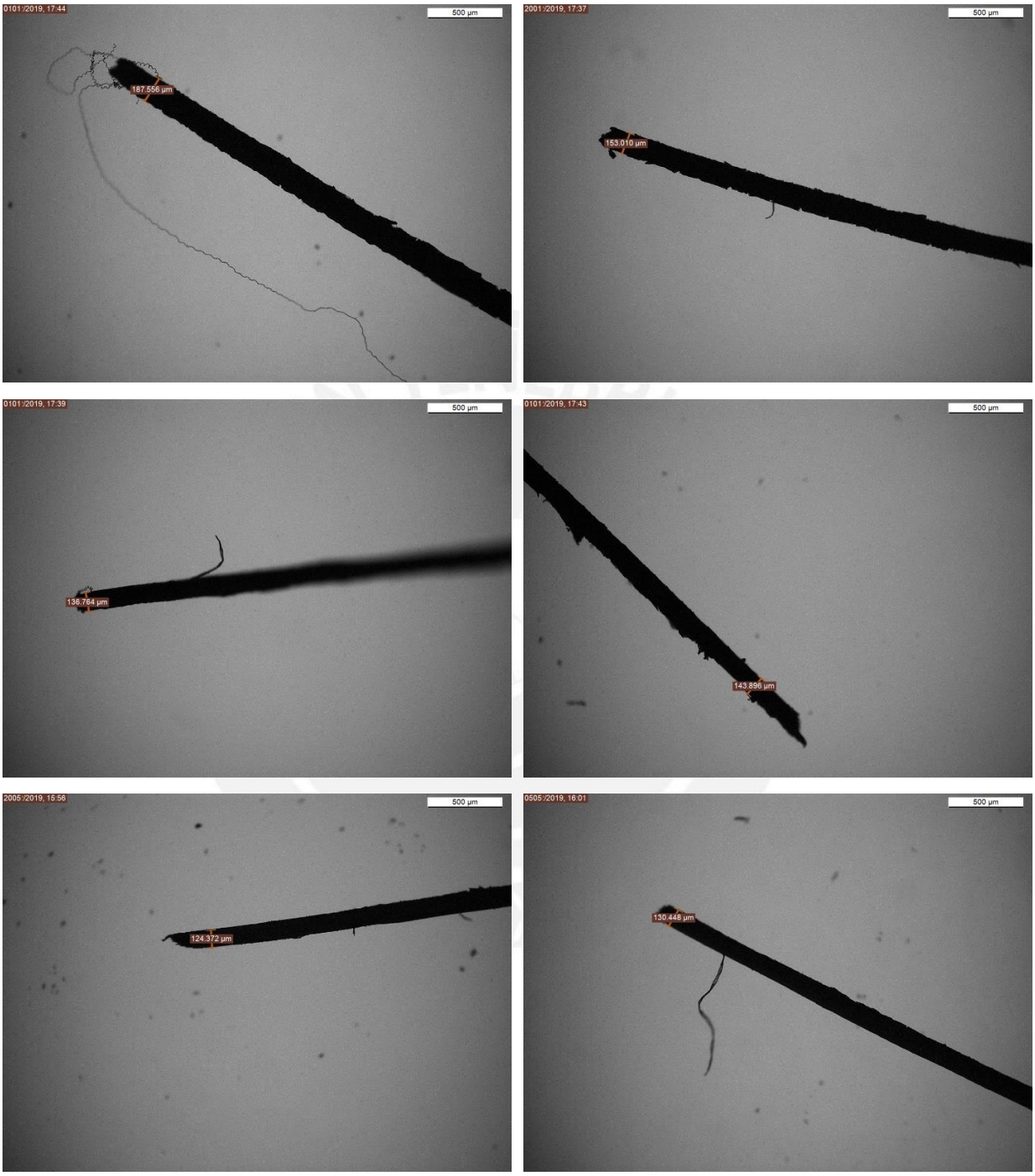

Measurement of the fiber diameter after the tensile strength test

I.B. Mechanical test for *Agave americana* fibers

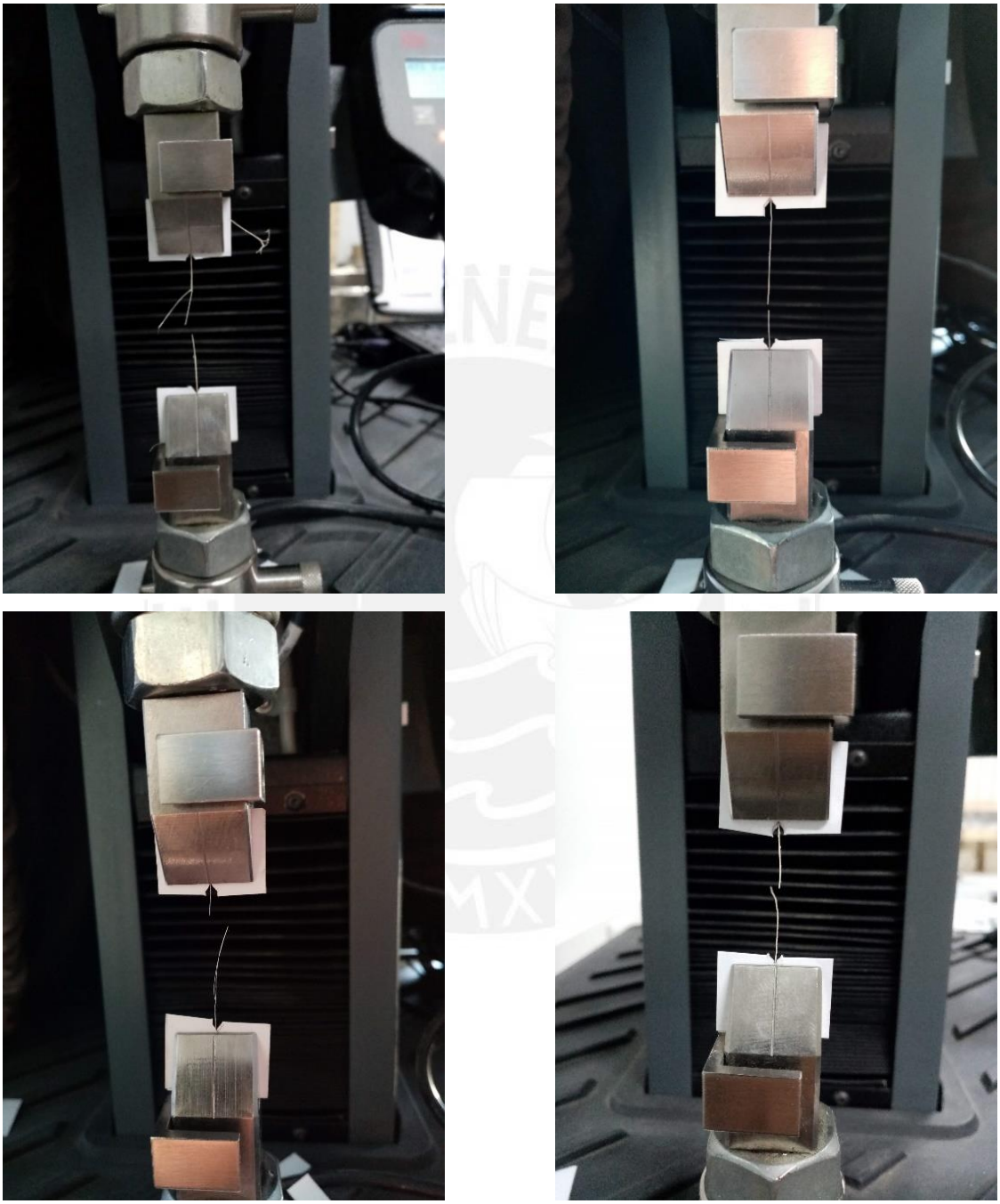

Tensile strength samples after test

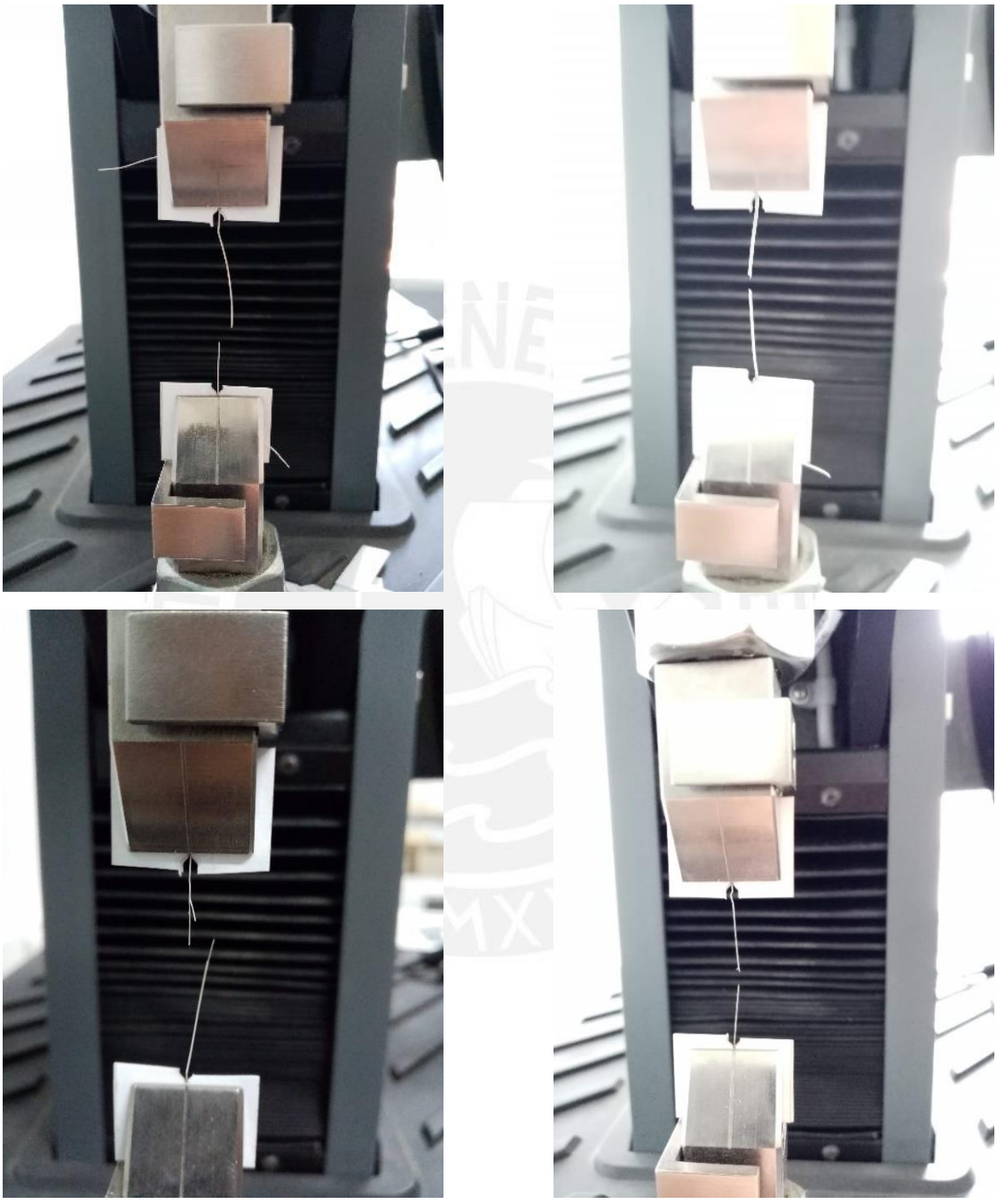

Tensile strength samples after test

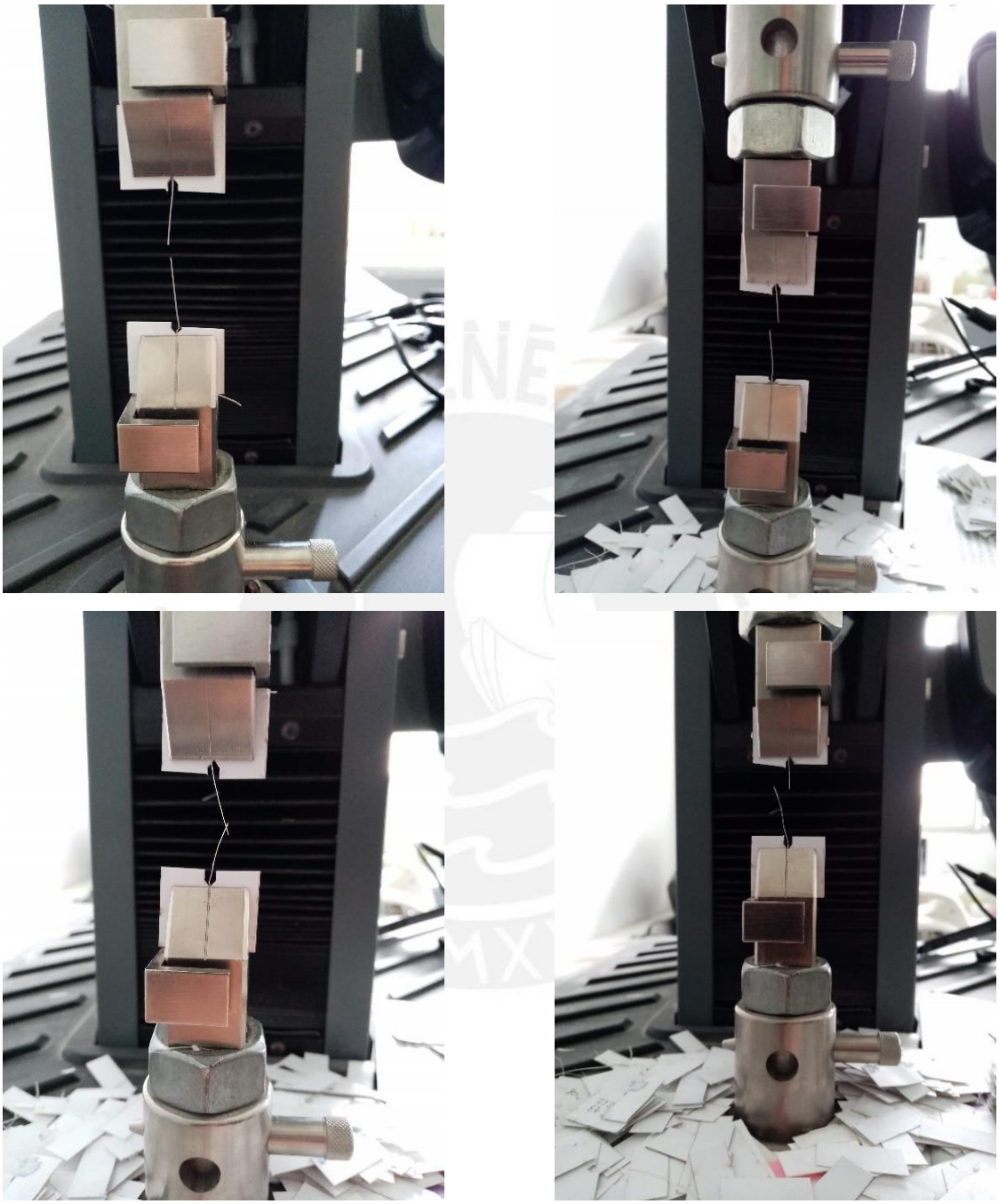

Tensile strength samples after test

APPENDIX II: Chapter 5 –Photos of the experimental stage

II.A. Mechanical test for control geopolymers

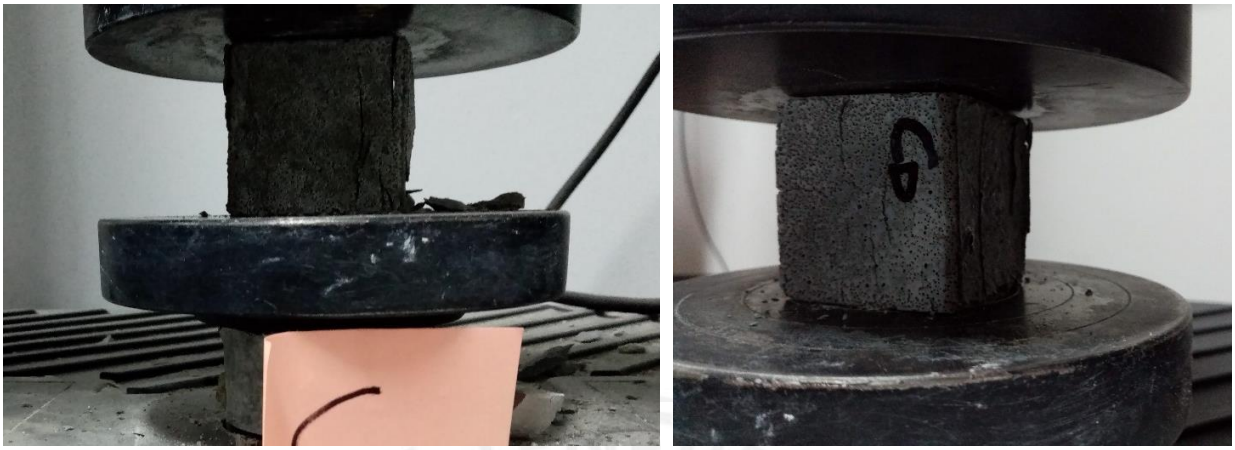

Compressive strength samples after test

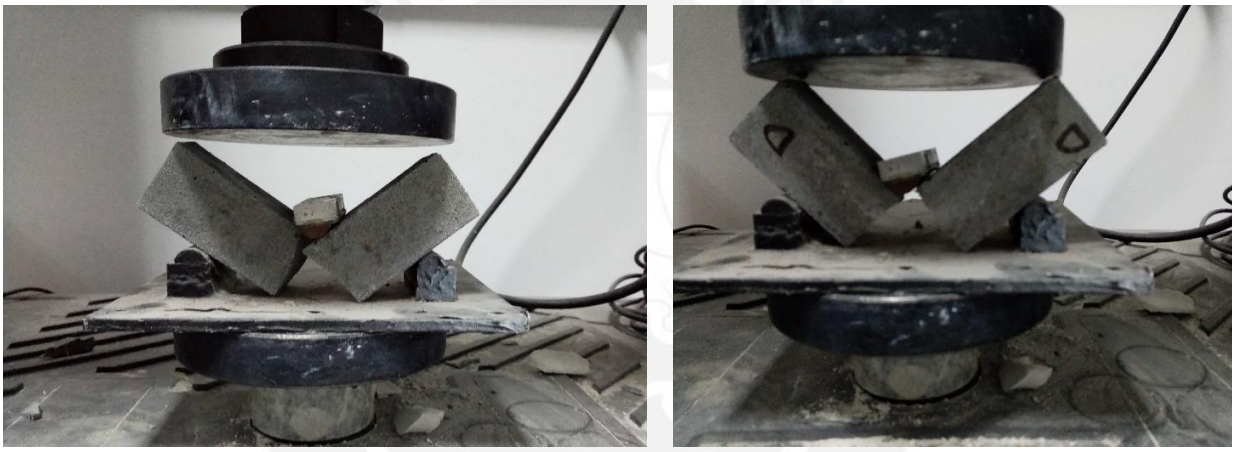

Flexural strength specimens after test

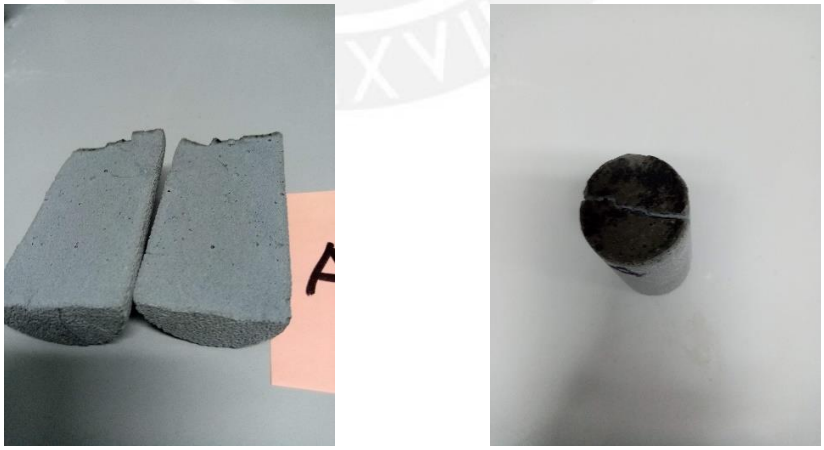

Splitting tensile strength specimens after test

II.B. Mechanical test for the reinforced geopolymers with 0.5% fiber content

Compressive strength samples after test

Flexural strength specimens after test

Splitting tensile strength specimens after test

II.C. Mechanical test for the reinforced geopolymers with 0.75% fiber content

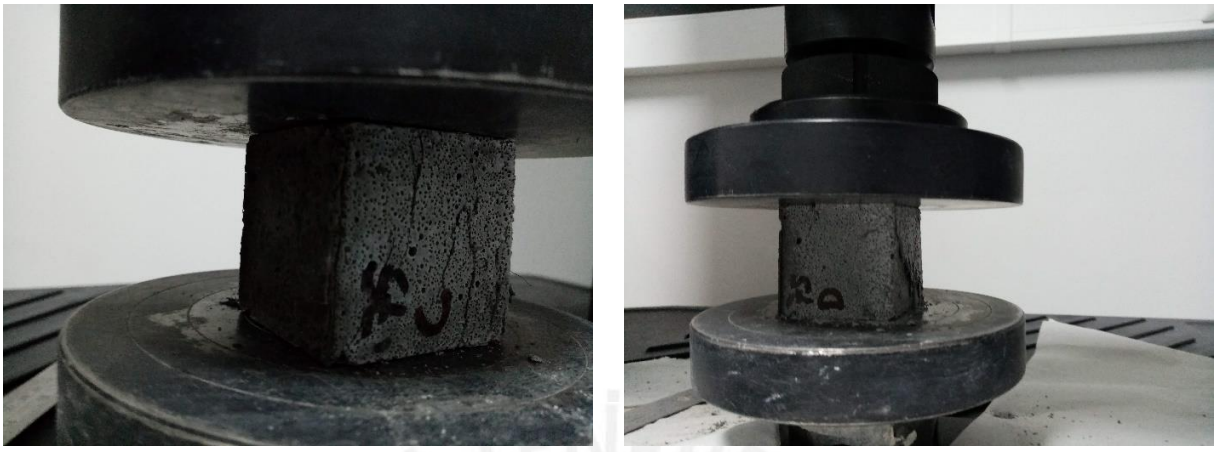

Compressive strength specimens after test

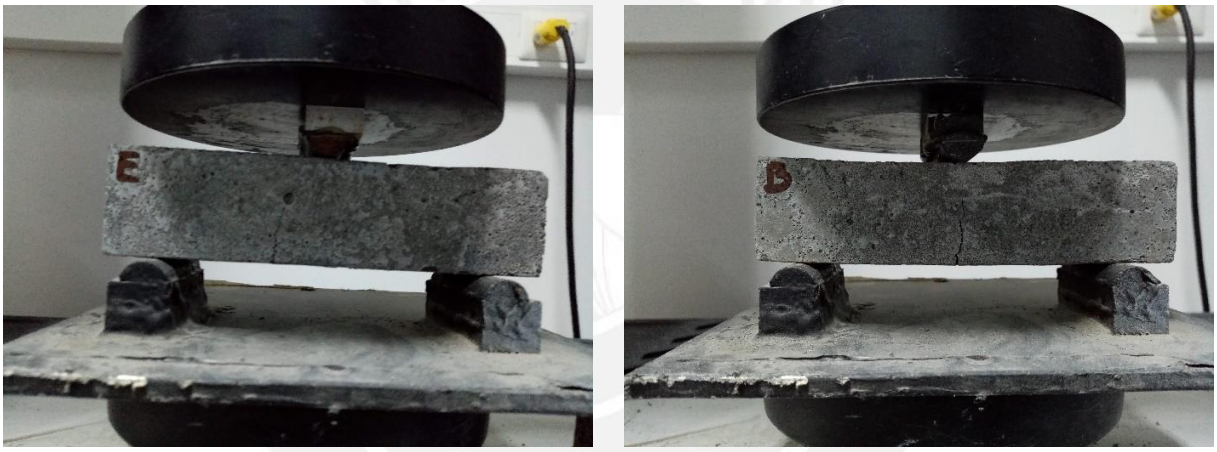

Flexural strength specimens after test

Splitting tensile strength specimens after test

II.D. Mechanical test for the reinforced geopolymers with 1% fiber content

Compressive strength specimens after test

Flexural strength specimens after test

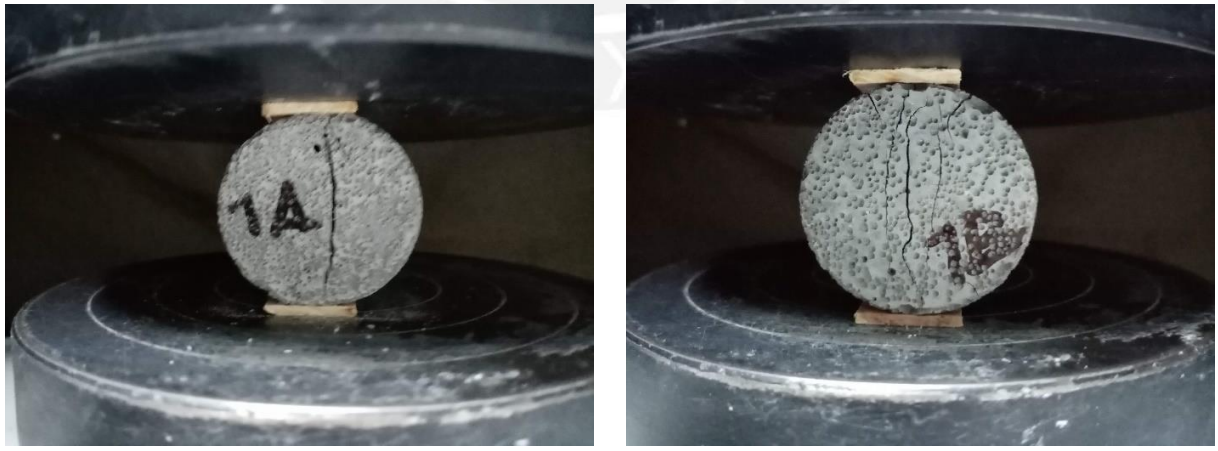

Splitting tensile strength specimens after test